Reactive-Transport Simulation of Phosphorus in the Sewage Plume at the Massachusetts Military Reservation, Cape Cod, Massachusetts

By DAVID L. PARKHURST, KENNETH G. STOLLENWERK, and JOHN A. COLMAN

Water-Resources Investigations Report 03-4017

TOXIC SUBSTANCES HYDROLOGY PROGRAM

In cooperation with the
AIR FORCE CENTER FOR ENVIRONMENTAL
EXCELLENCE

Northborough, Massachusetts
2003

U.S. DEPARTMENT OF THE INTERIOR

GALE A. NORTON, *Secretary*

U.S. GEOLOGICAL SURVEY

Charles G. Groat, *Director*

For additional information write to:

Chief, Massachusetts-Rhode Island District
U.S. Geological Survey
10 Bearfoot Road
Northborough, Massachusetts 01532

or visit our Web site at
http://ma.water.usgs.gov

Copies of this report can be purchased from:

U.S. Geological Survey
Branch of Information Services
Box 25286, Federal Center
Denver, CO 80225-0286

CONTENTS

FIGURES

TABLES

CONVERSION FACTORS, VERTICAL DATUM, ABBREVIATIONS, AND ACRONYMS

CONVERSION FACTORS

Multiply	By	To obtain
centimeter (cm)	0.3937	inch
gram (g)	0.03527	ounce, avoirdupois
kilometer (km)	0.6214	mile
meter (m)	3.281	foot
meters per day (m/d)	3.281	foot per day
meters per second (m/s)	3.281	foot per second
milliliter (mL)	0.0002642	gallon
millimeter (mm)	0.03937	inch
million gallons per day (Mgal/d)	0.003785	cubic meters per day

VERTICAL DATUM

Sea level: Vertical coordinate information is referenced to the North American Vertical Datum of 1929 (NGVD29).

ABBREVIATIONS AND ACRONYMS

g/L	grams per liter
kg/yr	kilograms per year
MMR	Massachusetts Military Reservation
µm	micrometer
µmol/L	micromoles per liter
m^2/g	square meter per gram
m^2/L	square meter per liter
USGS	U.S. Geological Survey

Reactive-Transport Simulation of Phosphorus in the Sewage Plume at the Massachusetts Military Reservation, Cape Cod, Massachusetts

By David L. Parkhurst, Kenneth G. Stollenwerk, *and* John A. Colman

ABSTRACT

The subsurface transport of phosphorus introduced by the disposal of treated sewage effluent to ground-infiltration disposal beds at the Massachusetts Military Reservation on western Cape Cod was simulated with a three-dimensional reactive-transport model. The simulations were used to estimate the load of phosphorus transported to Ashumet Pond during operation of the sewage-treatment plant—from 1936 to 1995—and for 60 years following cessation of sewage disposal. The model accounted for spatial and temporal changes in water discharge from the sewage-treatment plant, ground-water flow, transport of associated chemical constituents, and a set of chemical reactions, including phosphorus sorption on aquifer materials, dissolution and precipitation of iron- and manganese-oxyhydroxide and iron phosphate minerals, organic carbon sorption and decomposition, cation sorption, and irreversible denitrification.

The flow and transport in the aquifer were simulated by using parameters consistent with those used in previous flow models of this area of Cape Cod, except that numerical dispersion was much larger than the physical dispersion estimated in previous studies. Sorption parameters were fit to data derived from phosphorus sorption and desorption laboratory column experiments. Rates of organic carbon decomposition were adjusted to match the location of iron concentrations in an anoxic iron zone within the sewage plume. The sensitivity of the simulated load of phosphorus transported to Ashumet Pond was calculated for a variety of processes and input parameters.

Model limitations included large uncertainties associated with the loading of the sewage beds, the flow system, and the chemistry and sorption characteristics in the aquifer. The results of current model simulations indicate a small load of phosphorus transported to Ashumet Pond during 1965–85, but this small load was particularly sensitive to model parameters that specify flow conditions and the chemical process by which non-desorbable phosphorus is incorporated in the sediments. The uncertainties were large enough to make it difficult to determine whether loads of phosphorus transported to Ashumet Pond in the 1990s were greater or less than loads during the previous two decades.

The model simulations indicate substantial discharge of phosphorus to Ashumet Pond after about 1965. After the period 2000–10 the simulations indicate that the load of phosphorus transported to Ashumet Pond decreases continuously, but the load of phosphorus remains substantial for many decades. The current simulations indicate a peak in phosphorus

discharge to Ashumet Pond of about 1,000 kilograms per year during the 1990s; however, comparisons of simulated phosphorus concentrations with measured concentrations in 1993 indicate that the peak in phosphorus load transported to Ashumet Pond may be larger and moving more quickly in the model simulations than in the aquifer.

The results of the three-dimensional reactive-transport simulations are consistent with the loading history, experimental laboratory data, and field measurements. The results of the simulations adequately reproduce the spatial distribution of phosphorus concentrations measured in 1993, the magnitude of changes in phosphorus concentration with time in a profile near the disposal beds following cessation of sewage disposal, the observed iron zone in the sewage plume, the approximate flow of treated sewage effluent into Ashumet Valley, and laboratory-column data for phosphorus sorption and desorption.

INTRODUCTION

Secondarily treated sewage effluent was discharged from 1936 to 1995 to sand beds at the Massachusetts Military Reservation (MMR), Cape Cod, Massachusetts, which is on a broad, glacial outwash plain on western Cape Cod (LeBlanc, 1984; Walter and others, 1996). The disposal of treated sewage effluent has created a plume of sewage-contaminated ground water in the local aquifer that has moved southward to Ashumet Pond and into Ashumet Valley (fig. 1). Disposal of treated sewage effluent ended in 1995, but effects of the long-term disposal operations remain (LeBlanc and others, 1999).

At the time of cessation of sewage disposal, phosphorus concentrations were greatest in that part of the plume just downgradient from the southeastern disposal beds—between the beds and Ashumet Pond (fig. 2, Walter and others, 1996). The elongation of the phosphorus-concentration contours toward Ashumet Pond indicates flow from the disposal beds toward Ashumet Pond. Ground-water flow directions in the aquifer (Walter and others, 1996) also show that ground water flows from the southeastern disposal beds to Ashumet Pond. However, the flow directions indicate that ground-water flow from the western disposal beds skirts the Pond and moves down Ashumet Valley (fig. 3). Flow directions in the vicinity of Ashumet Pond may vary by as much as 15° (Walter and others, 1996).

The magnitude of the phosphorus load transported to Ashumet Pond directly affects the health of the pond ecosystem. Estimates of the past and future loads of phosphorus are thus important information for planning a management strategy for Ashumet Pond. To address these needs and other environmental issues, the U.S. Geological Survey, in cooperation with the Air Force Center for Environmental Excellence, has studied the distribution and transport of phosphorus and other contaminants in the sewage plume at the MMR.

PURPOSE AND SCOPE

The purpose of this report is to describe a reactive-transport model that was developed to simulate phosphorus in the sewage plume at the MMR. Loads of phosphorus transported to Ashumet Pond were simulated over the course of the sewage-treatment-plant operation at MMR and over a 60-year time period after cessation of sewage disposal. The simulated phosphorus loads transported to Ashumet Pond are needed to formulate effective management strategies for Ashumet Pond. The report describes the selection of a set of chemical reactions for phosphorus and cation sorption, sorption and degradation of organic carbon, sequestration of non-desorbable phosphorus, and mineral equilibria; the evaluation of parameters for phosphorus and cation sorption to aquifer sediments by using data from laboratory-column experiments; the estimation of the rate of organic degradation reactions in the sewage plume; the testing of the sensitivity of the model to model parameters; the comparison of measured phosphorus

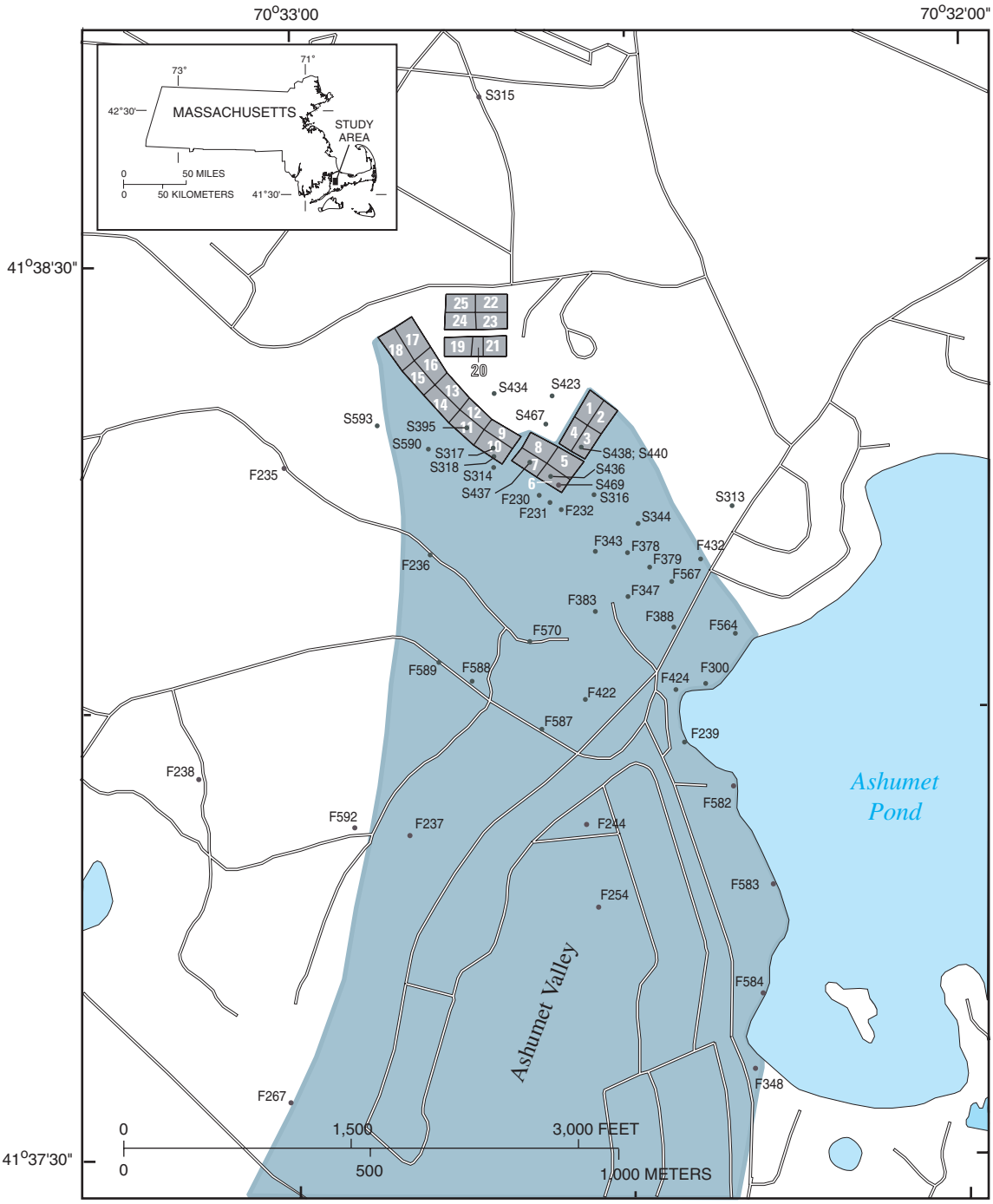

Modified from Savoie and LeBlanc (1998)

EXPLANATION

- SEWAGE PLUME
- 1 — SEWAGE DISPOSAL BEDS AND IDENTIFIERS
- F254 — WELL-CLUSTER SITES AND LOCAL IDENTIFIERS

Figure 1. Location of disposal beds in the study area at the Massachusetts Military Reservation sewage-treatment plant near Ashumet Pond, Massachusetts, and extent of the sewage plume in Ashumet Valley as of 1993–94.

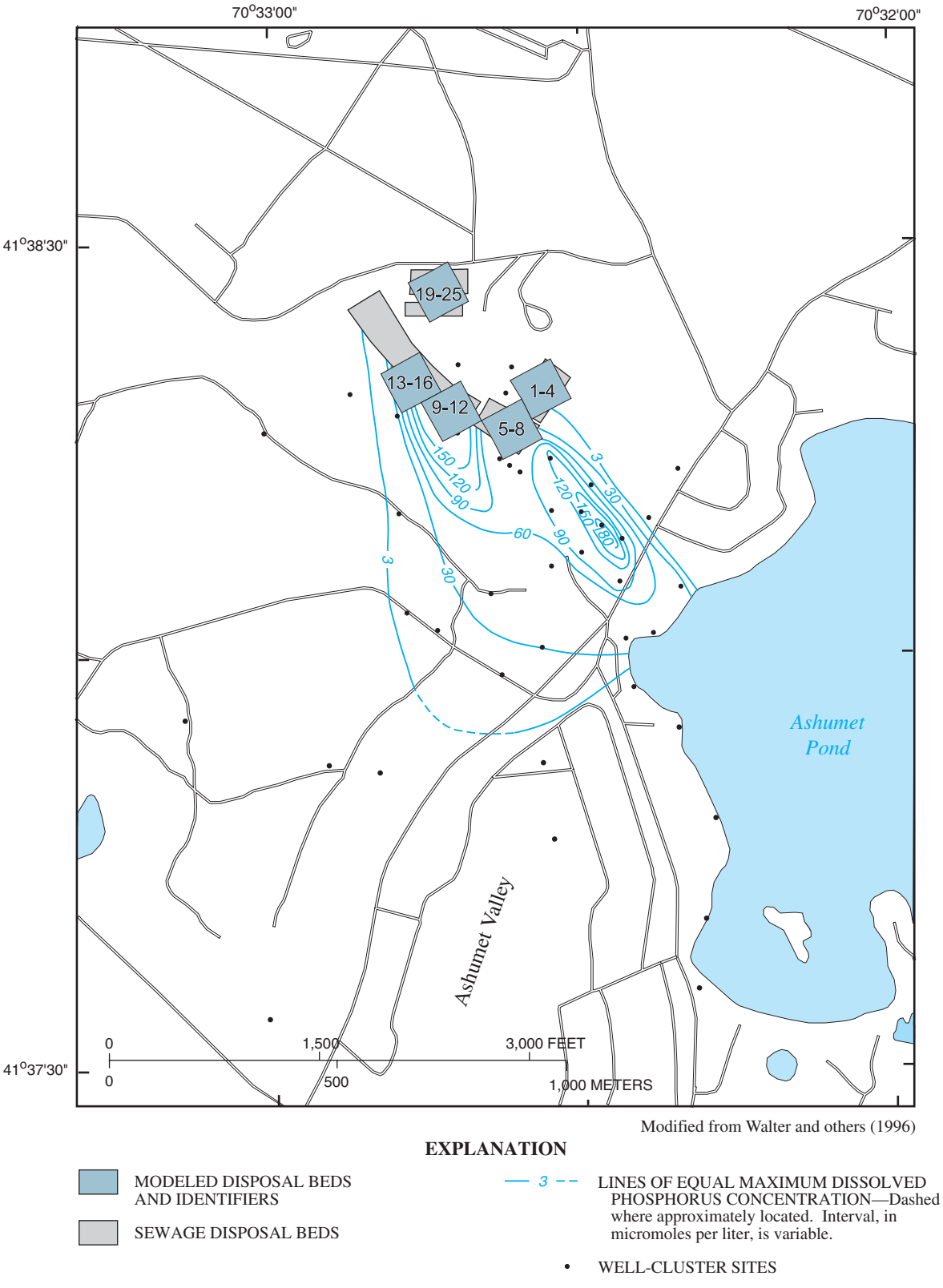

Figure 2. Areal distribution of maximum dissolved phosphorus concentrations in ground water near Ashumet Pond, Massachusetts, August to November 1993.

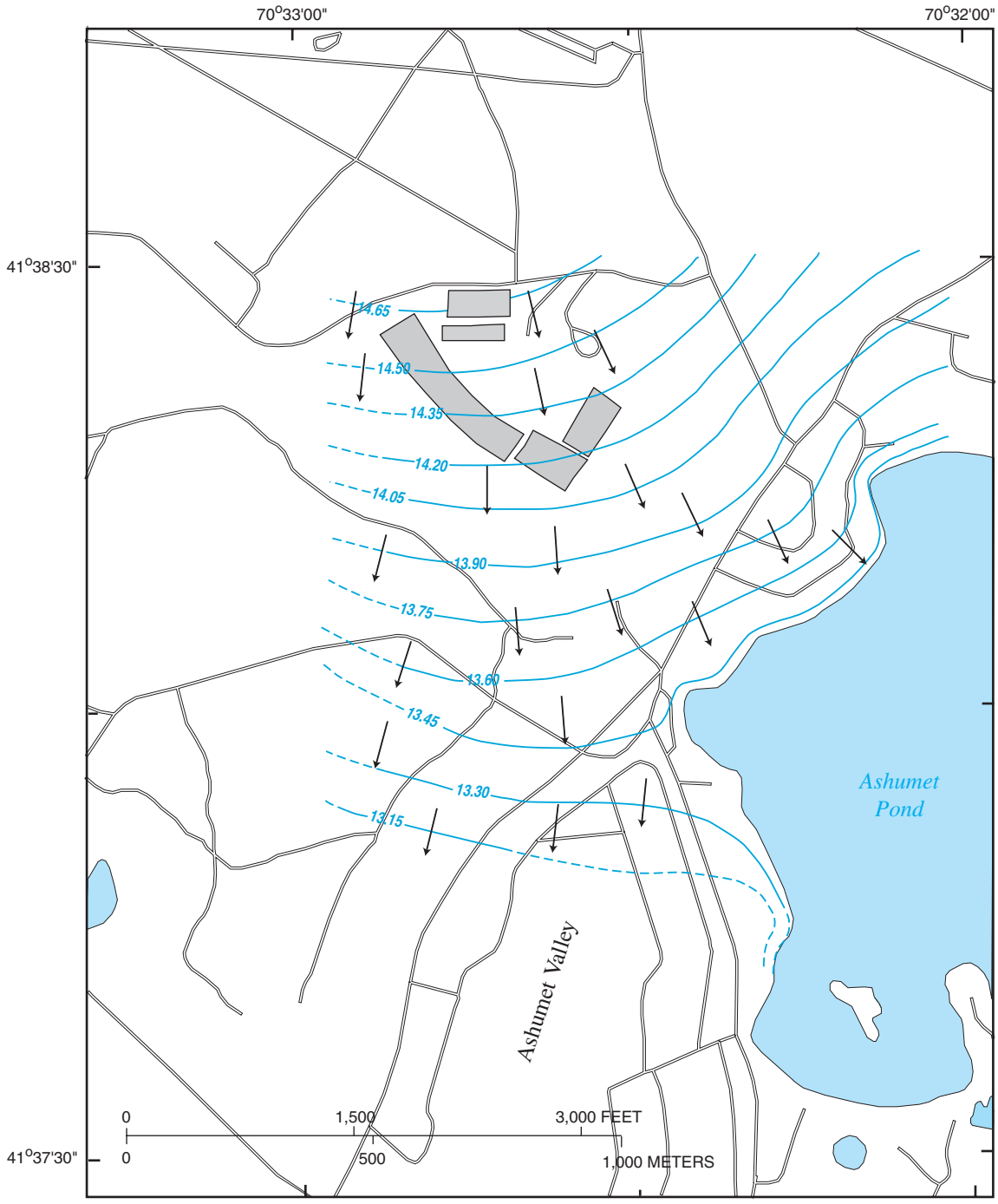

Modified from Walter and others (1996)

EXPLANATION

SEWAGE DISPOSAL BEDS

13.45 WATER-TABLE CONTOURS—Show altitude of water table. Dashed where approximately located. Contour interval is 0.15 meter. Datum is NGVD29.

APPROXIMATE DIRECTION OF GROUND-WATER FLOW

Figure 3. Altitude of the water table and approximate direction of ground-water flow in January 1994 near Ashumet Pond, Massachusetts.

concentrations to simulated phosphorus concentrations; and the estimation of the loads of phosphorus transported to Ashumet Pond.

A base-case model was developed on the basis of chemical analyses of samples taken from the aquifer in 1993, ground-water data from 1996, and results from laboratory-column experiments. A revised model was then developed by the inclusion of additional chemical processes and by the adjustment of the base-case model parameters on the basis of sensitivity simulations and comparisons with additional laboratory-column experiments. The reactive-transport simulations produced results for dissolved concentrations of each major element plus nitrogen, phosphorus, dissolved organic carbon, pH, and redox conditions; sorbed concentrations of phosphorus and major cations; and concentrations of solid constituents—iron and manganese oxyhydroxides, iron-phosphate minerals, and sorbed organic carbon. For the purposes of this report, only the simulation results for phosphorus are discussed in detail.

METHODS

This section describes a three-dimensional reactive-transport model used to simulate transport of phosphorus downgradient from the disposal beds at the MMR. Model definitions include geometry and boundary conditions, initial conditions, and selection of chemical reactions. A description of computer resources used for the simulations is provided. Finally, this section describes experimental methods for laboratory experiments to determine phosphorus sorption and desorption from sediment columns and numerical methods for the determination of equilibrium constants from the column-experiment results.

Reactive-Transport Model

The modeling described in this report expands on previous work by Stollenwerk and Parkhurst (1999) in which PHREEQC, a one-dimensional model, was used to simulate reactive transport in the sewage plume. Because of the simple mineralogy and the rapidity of the flow system in the aquifer in the vicinity of the MMR, few reactions need to be considered in a reactive-transport model of phosphorus. Carbonate minerals are absent from the aquifer sediment, and the primary minerals that compose the sediments—quartz and feldspars (Barber, 1990)—are relatively inert on the time scale of the flow system. Minor amounts of glauconite and clay minerals are present (Barber, 1990), which allow for a small amount of cation exchange or sorption. Iron and manganese oxyhydroxide minerals and coatings of the aquifer sediments can be assumed to react rapidly under anoxic conditions. Iron and aluminum oxyhydroxide minerals provide large surface areas that can reversibly sorb phosphate and other ions, and can buffer the pH of the ground water to a significant extent. Phosphate can be sequestered in iron and aluminum oxyhydroxide minerals as solid solutions or in authigenic iron and aluminum phosphate minerals.

The chemical reactions in the contaminated part of the aquifer are driven primarily by the loading of treated sewage effluent. The phosphorus in the effluent is the source of the phosphorus plume in the aquifer. Organic carbon introduced with the effluent enters the ground-water system and is readily reactive, but this organic carbon also may sorb on aquifer sediments and continue to react over an extended period of time. All of the reactions that occur rapidly can affect the transport of phosphate, in large part because they affect the pH of the ground water. The buffering of pH by these reactions directly affects the sorption of phosphorus and the formation of phosphate minerals.

Reactive-transport models are a recent development and modelers do not have a large body of work from which to draw. The combined capability to model flow, transport, and chemical reactions provides a systematic approach for studying ground-water processes. The model developed in this report attempts to include all of the significant processes affecting the transport of phosphorus to Ashumet Pond and to provide a comprehensive description of the evolution of ground-water and sediment chemistry. Even though large uncertainties are associated with the modeling results, a reactive-transport model is the only systematic method available to estimate the time dependency of the loads of phosphorus transported to Ashumet Pond and to assess the sensitivity of the load estimate to various chemical and physical processes.

The three-dimensional reactive-transport model used to develop the base-case and revised models was PHAST (Parkhurst and others, 1995; Parkhurst and Kipp, 2002). PHAST couples capabilities to simulate ground-water flow and associated solute transport with

the capability to simulate chemical reactions. The ground-water flow and transport parts of PHAST are derived from HST3D (Kipp, 1997) and the chemical reaction part of the model is derived from PHREEQC (Parkhurst and Appelo, 1999). In this study, PHAST was used (1) to estimate sorption properties of the aquifer sediments, (2) to estimate the rate constant for organic decomposition reactions in the aquifer, and (3) to simulate the evolution of the sewage plume over time, specifically, to calculate loads of phosphorus transported to Ashumet Pond.

The hydraulic parameters and boundary conditions for the three-dimensional reactive-transport model were taken from models developed for previous studies (LeBlanc, 1984; LeBlanc and others, 1991; Garabedian and others, 1991; Walter and others, 1996; Masterson and Walter, 2000). Although the USGS computer code MODFLOW (McDonald and Harbaugh, 1988; Harbaugh and McDonald, 1996) was used to simulate ground-water flow in these studies, PHAST solves the same partial differential flow equations as MODFLOW and uses the same hydraulic parameters. Simulated ground-water heads for the model domain used in this study were not adjusted by modifying parameters in a formal calibration procedure, but the simulated heads used in this study approximate heads simulated for previous studies. The flow system simulated by PHAST approximates the flow system in the aquifer in the study area and is appropriate for the reactive-transport simulations described in this report.

Computer Resources

Calculations for the reactive-transport simulations described in this report were run with a parallel-computing version of PHAST on a Beowulf cluster with up to 14 dual-processor personal computers. Individual processor speeds ranged from 0.5 to 1.8 gigahertz and each computer had 0.75 or 1.0 gigabytes of memory. Local-area-network connection was by dual 100-megabit Ethernet with an effective data-transfer rate of about 150 megabits per second. The parallel-computing version of PHAST (Parkhurst and Kipp, 2002) used a single processor to run the flow and transport calculations, whereas the chemical calculations for the nodes were distributed among the available processors with a load-balancing strategy. Calculations for the base-case model required about two hours of elapsed time on a cluster of 20 processors.

Column Experiments

Sorption/desorption column experiments (Stollenwerk, 1996) were performed with pristine sediments unaffected by sewage effluent to evaluate phosphorus and cation-sorption parameters, which included equilibrium constants for sorption of phosphorus, cations, and hydrogen ion, and the concentration of sorption sites for phosphorus and cations. Desorption column experiments in which phosphorus was leached from contaminated sediment were simulated with PHAST to test the validity of the sorption parameters for simulating desorption of phosphorus from sewage-contaminated sediments in contrast to sorption and desorption from pristine sediments.

Sorption/Desorption Column Experiments

The sorption/desorption column experiments were designed to evaluate sorption and desorption of phosphorus from uncontaminated aquifer sediment. Sediment was collected 1.3–1.6 m below land surface from a trench excavated in the unsaturated zone at a gravel pit about 200 m south of the sewage disposal beds. Previous studies have shown that sorption properties of this sediment are similar to sediment from the saturated zone (Stollenwerk, 1995).

Uncontaminated ground water was collected from a well that was screened above the sewage plume. Sewage-contaminated ground water was collected from a well that was screened in the suboxic zone of the sewage plume. Unfiltered ground water was collected in polyethylene bottles that were stored in ice during shipment. All water was filtered in the laboratory through a 0.4-μm pore-size, polycarbonate-membrane filter and refrigerated until needed. The suboxic ground water became saturated with oxygen during the experiments; however, because some oxygen was already present in the ground water and the experiments remained oxic throughout, the additional dissolved oxygen introduced by air equilibration is expected to have had little effect on the experiment.

Replicate Plexiglas columns, approximately 30 cm in length with 2.5-cm inside diameter, were filled with the homogenized fraction of the sediment sample less than 2 mm in size. This size fraction accounted for 90 percent by weight of the sediment. A peristaltic pump was used to drive solutions through the columns at a velocity of about 0.4 m/d, which is approximately the velocity of ground water in this part of the aquifer. Leachate was collected in a fraction collector that was sealed and humidified to minimize evaporation. Pre-sewage-plume conditions were established by rinsing columns with uncontaminated ground water until the chemistry of the column leachate stabilized at that of the eluent. A bromide tracer was then added to estimate longitudinal dispersivities of the columns for transport simulations.

After the bromide was eluted from the columns, the eluent solution was changed to sewage-contaminated ground water. One set of experiments used the phosphorus concentration of 16 µmol/L that was present in the sewage-contaminated ground water collected for the experiment. In a second set of experiments, this ground water was spiked to 196 µmol/L phosphorus. The two concentrations represent the range of phosphorus concentrations measured in contaminated ground water in the plume. Sewage-contaminated ground water was eluted through the columns until the leachate concentration of phosphorus approached the eluent concentration. The eluent solution was changed to uncontaminated ground water after 115 pore volumes for the 16-µmol/L experiment and after 48 pore volumes for the 196-µmol/L experiment to evaluate desorption.

Fitting Surface-Sorption Parameters from Sorption/Desorption Experimental Data

PHAST was used to simulate flow and chemical reactions for the sorption/desorption column experiments. A version of the parameter-estimation code, UCODE (Poeter and Hill, 1999), modified to use multiple computer processors, was used to fit chemical parameters for phosphorus and cation sorption on aquifer sediments.The pH and phosphorus concentration in the column leachate were fit by adjusting surface-complexation parameters. The data included 432 phosphorus and 180 pH analyses from column 1 (16-µmol/L phosphorus eluent) and 135 phosphorus and 31 pH analyses from column 3 (196-µmol/L phosphorus eluent). The phosphorus data were weighted by using a standard deviation equal to the square root of the concentration (µmol/L) for each point, or 0.1 if the analysis was below the detection limit of the chemical analytical method; the pH data were weighted by using a standard deviation of 0.2 for each point.

Table 1 lists properties of the column used in phosphorus sorption/desorption experiments. Length and porosity were measured. Mass of solid per liter of water was calculated by using an estimated density of 2,650 g/L for solids and porosity of 0.33 to give 5,380 g solid/L water. Surface area per liter of water was calculated by using an average measured specific surface area of 0.3 m^2/g solid (Stollenwerk, 1995).

Iron- and manganese-oxyhydroxide minerals were specified to be present in the uncontaminated aquifer in concentrations representative of those measured by chemical extraction of the solids, 80,000 µmol/L of iron oxyhydroxide and 700 µmol/L of manganese oxide (Coston and others, 1995). Ferric hydroxide was chosen as the representative iron phase, which was assumed to react to equilibrium with the aqueous phase throughout the simulations. The equilibrium constant for amorphous ferric hydroxide was taken from the *phreeqc.dat* database of PHREEQC [$Fe(OH)_3(a)$] (Parkhurst and Appelo, 1999). Pyrolusite was chosen as the representative manganese oxide and was assumed to react to equilibrium with the aqueous phase, unless the mineral was completely removed by dissolution. The equilibrium constant for pyrolusite in the database *phreeqc.dat* was used for all simulations (Parkhurst and Appelo, 1999).

Phosphorus sorption was modeled as a surface-complexation process (Dzombak and Morel, 1990; Parkhurst and Appelo, 1999, p. 28–29) that proceeds by the reaction:

$$SiteOH + PO_4^{3-} + 2H^+ = SiteHPO_4^- + H_2O, \quad (1)$$

where $Site$ represents a phosphorus-sorption site on the aquifer solids. The surface complexation mass-action equation includes an electrostatic term to account for the work done in moving a charged species to the charged surface (Parkhurst and Appelo, 1999, p. 14–15). The equilibrium constant for this reaction was fit to the data from the sorption/desorption column experiments. Although many different combinations of chemical sorption reactions and physical parameters were tried, the final fits were made by using equation 1. No competing anion sorption reactions were considered for phosphorus sorption, except for protonation and deprotonation of the sorption site.

Table 1. Properties used in reactive-transport simulation of the phosphorus sorption/desorption column experiments

[g/L, grams per liter; m, meter; µmol/L, micromoles per liter; m^2/g, square meter per gram]

Column properties	Value
Length, m	0.3
Porosity, unitless	.33
Density of solid, g/L solid	2,650
Mass of solid per liter of water, g/L water	5,380
Surface area, m^2/g solid	.3
Surface area, m^2/L water	1,614
$Fe(OH)_3(a)$, µmol/L water	80,000
MnO_2, µmol/L water	700

Table 2. Composition of synthetic ground water used in phosphorus desorption column experiment

[Concentrations are in micromoles per liter, except for pH, in standard units]

Constituent	Concentration
pH	5.78
Calcium	72
Magnesium	33
Sodium	240
Potassium	62
Chloride	370
Sulfate	45
Bicarbonate	80
Phosphorus	<.6
Iron	<.05

Phosphorus Desorption Experiments

In the desorption column experiment, the desorbable fraction of phosphorus associated with sewage-contaminated sediment was measured. The purpose was two-fold: (1) to evaluate desorption of phosphorus from sediment that had been exposed to sewage effluent for many years, in contrast to desorption measured during the sorption/desorption experiments, which involved pristine sediments exposed to sewage-contaminated water for less than 90 days, and (2) to test the accuracy of the model parameters for simulating phosphorus desorption from sewage-contaminated aquifer sediments. Cores were collected in April 2000 from contaminated parts of the aquifer downgradient from the disposal beds. A total of 17 cores was collected in plastic liners from locations between the disposal beds and Ashumet Pond. The cores were stored on ice during shipment and refrigerated until needed. The only desorption column experiment described in this report is for the core collected from site S469 at the southern edge of the disposal beds (site S469 in fig. 1). This core was collected from a depth of 15.5–15.9 m above NGVD29. The 33-cm-long core was fitted with endcaps containing inlet and outlet ports. Synthetic ground water that was representative of the major-ion composition of uncontaminated ground water in the aquifer (table 2) was eluted through the core. Measured porosity was 0.3 and an average flow velocity of 0.4 m/d was used (range = 0.3–0.5 m/d). Initially the eluent pH was set at 5.78; after 50 pore volumes, the eluent pH was increased to 7.42; and after 150 pore volumes, the eluent pH was decreased back to 5.78.

The reason for the pH changes was to evaluate the changes in phosphorus concentrations in response to changes in eluent pH. Phosphorus concentration and pH of the leachate were monitored throughout the experiments.

Desorption of phosphorus in the experiment with sewage-contaminated sediment is more representative of processes occurring in the aquifer after cessation of sewage disposal than the sorption/desorption column experiment with pristine sediment. However, the desorption experiments require several months to run. To obtain data from a larger number of core samples in a reasonable time frame, batch desorption experiments were conducted at pH of 10. A pH of 10 is high enough to maximize phosphorus desorption, yet low enough to minimize dissolution of iron and aluminum oxides, the principal sorbents for phosphorus in this aquifer.

Total desorbable and acid-extractable phosphorus were measured in samples from all 17 cores. For total desorbable phosphorus at pH of 10, 15 g of wet core material was equilibrated with 25 mL of uncontaminated ground water in 40-mL polyethylene centrifuge tubes, and pH was adjusted to 10 with NaOH. Experiments were run in triplicate. The suspensions were equilibrated for 2 days on an end-over-end rotating mixer and then centrifuged for 20 minutes at 15,000 revolutions per minute. The centrifugate was analyzed for phosphorus and pH. This process was repeated until phosphorus desorption became negligible, usually after eight extractions. The total concentration of phosphorus desorbed from each

core was then calculated. Total acid-extractable phosphorus was analyzed on separate splits of the core samples, and non-desorbable phosphorus was calculated by difference. For acid-extractable phosphorus, 15 g of wet core material was equilibrated with 25 mL of 1N HCl for 24 hours on an end-over-end rotating mixer and then centrifuged for 20 minutes at 15,000 revolutions per minute. These experiments were run in triplicate and involved only one extraction.

Analytical Methods

Phosphorus was analyzed by the phosphomolybdate colorimetric procedure (Fishman and Friedman, 1985). pH was measured with an Orion pH meter and Ross pH electrode. Cations were analyzed by inductively coupled atomic-emission spectroscopy; anions were analyzed by ion chromatography.

REACTIVE-TRANSPORT SIMULATIONS

This section describes the base-case model, results of fitting model parameters to the sorption/desorption experimental data, and a series of sensitivity simulations. A revised model is developed by making adjustments to the base-case model. The revised model was used to make estimates of the load of phosphorus transported to Ashumet Pond.

Base-Case Model

The MMR site and the underlying aquifer have been extensively studied over the last 20 years, and many of the hydraulic parameters for the aquifer are well known. Most of the hydraulic properties for the aquifer, chemical compositions of ground water and sewage effluent, and characteristics of the flow system were selected from previous studies of the aquifer (LeBlanc, 1984; LeBlanc and others, 1991; Garabedian and others, 1991; Walter and others, 1996; Masterson and Walter, 2000).

Chemical reactions and reaction parameters were estimated through interpretation of the column experimental data and concentration data from the aquifer.

Geometry of the Model Grid

In the vicinity of the MMR, water in the aquifer flows radially outward from a ground-water high about 5 km north of the sewage disposal beds (Masterson and Walter, 2000). The model for PHAST was chosen to simulate flow and transport in a region of the aquifer that includes the area of the sewage disposal beds, the northeast corner of Ashumet Pond, and the northern end of Ashumet Valley. An area 1,600 m in length that widens from 800 m at the northern end to 1,600 m at the downgradient southern end was chosen for the model domain (fig. 4). The widening area allows for spreading of the flow system, which is apparent in the water-table contours of figure 3 and is consistent with regional flow (Masterson and Walter, 2000). The eastern and western edges of the domain were chosen to align with the predominant flow directions (fig. 3). The eastern boundary is a straight line, whereas the western edge is stair-stepped progressively farther westward from north to south. The model domain is 45 m thick and extends from 30 m below NGVD29 to 15 m above NGVD29.

The model grid is a point-distributed mesh, such that the edges of the model are defined by nodes. Cell faces are placed halfway between nodes in each direction; for cells that border the exterior of the domain, cell faces coincide with the node. The model grid was discretized with 33 nodes at 50-m spacing in the X and Y directions, and 19 nodes at 2.5-m spacings in the Z direction (table 3). Each model simulation calculates a ground-water head and constituent concentrations at each of the nodes and a ground-water flux and constituent fluxes across each cell face at each time step.

The model grid is rotated counterclockwise relative to north and south by about 40 degrees. However, north, south, east, and west will be used to refer to the top, bottom, right, and left boundaries as shown on figure 4. The coordinate axes of the model grid are oriented so that positive X is south (the general direction of flow) and positive Y is east.

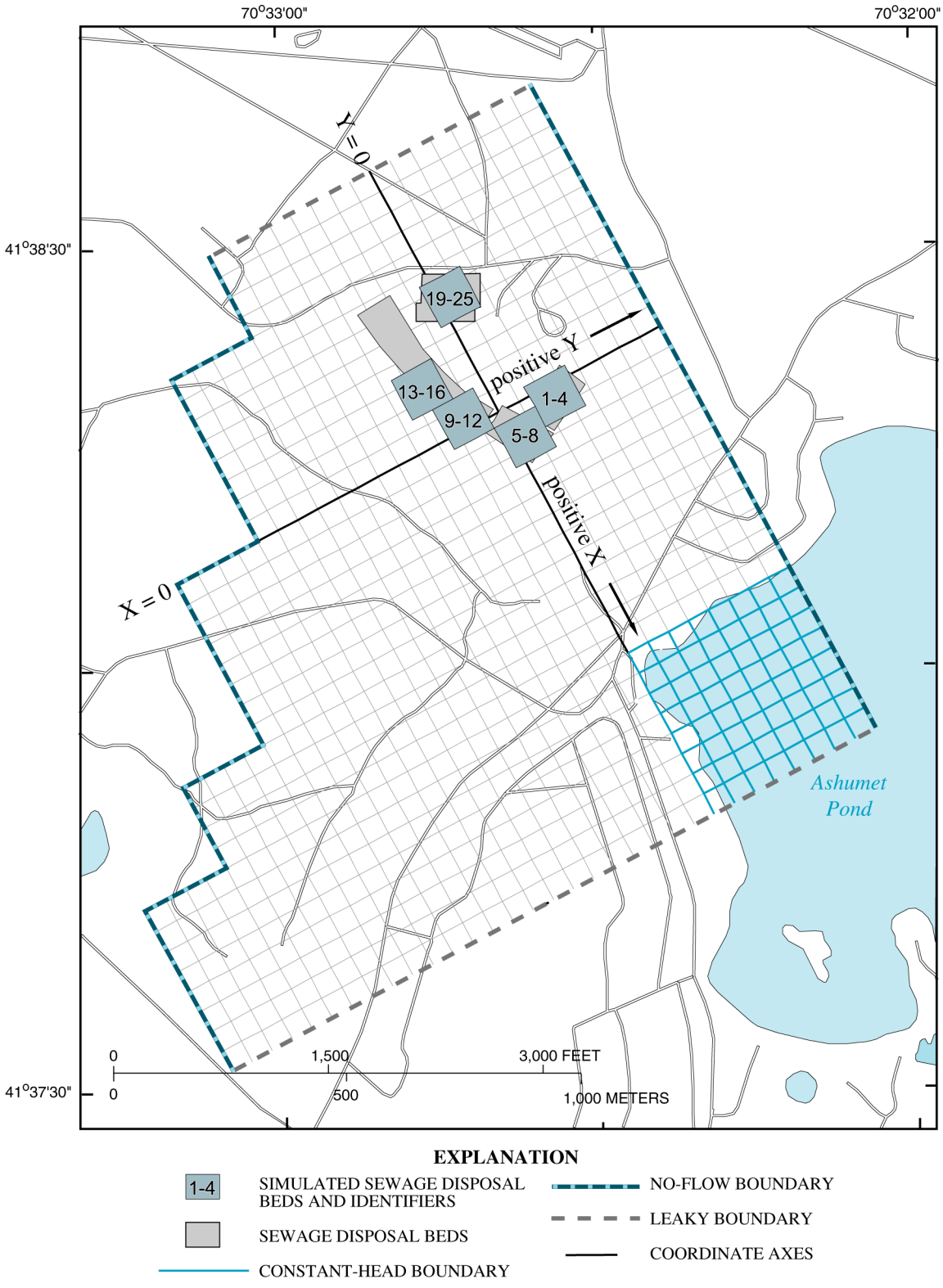

Figure 4. Model grid with 50-meter spacing for reactive-transport model of the area near Ashumet Pond, Massachusetts.

Table 3. Base-case parameters for three-dimensional reactive-transport modeling

[m, meters; m/d, meters per day; m/s, meters per second; yr, year]

Parameter	Value
Northern leaky boundary	
Distance to fixed head, m	1,700
Fixed head, m	18.3
Hydraulic conductivity for boundary, m/s	1.06×10^{-3}
Southern leaky boundary	
Distance to fixed head, m	800–1,300
Fixed head, m	12.19
Hydraulic conductivity for boundary, m/s	1.06×10^{-3}
Specified head for Ashumet Pond, m	13.42
Recharge, m/d	1.8×10^{-3}
Porosity	0.39
Hydraulic conductivity, m/s	
X - direction	1.06×10^{-3}
Y - direction	1.06×10^{-3}
Z - direction	0.3×10^{-3}
Grid dimensions	
X, m	50
Y, m	50
Z, m	2.5
Time step, yr	0.5
Estimated dispersivity, m	60

Hydraulic Properties

Hydraulic properties are listed in table 3.The hydraulic conductivity of the aquifer was specified to be 1.06×10^{-3} m/s in the horizontal direction and 0.3×10^{-3} in the vertical direction; the porosity was specified to be 0.39 (Garabedian and others, 1991). It is estimated that numerical dispersion in the model is far greater than the 1-m dispersivity measured in the tracer-test experiments carried out at locations within the area of interest (Garabedian and others, 1991). In the reactive-transport model, dispersivity was set to a small value (0.0001 m), so that numerical dispersion from the relatively large grid cells and time steps was the major cause of dispersion in the results. The numerical dispersivity is approximated by the following equation:

$$D = \frac{\Delta X}{2} + \frac{V \Delta T}{2}, \qquad (2)$$

where D is the numerical dispersivity (m), ΔX is the grid spacing in the X direction (m), ΔT is the time step (day), and V is velocity (m/day). The numerical dispersivity in the X direction (the predominant direction of flow) is approximately

$$\frac{50}{2} + \frac{0.4(180)}{2} \cong 60 \text{ m},$$

for 50-m grid cells and half-year (180-day) time steps. The effects of numerical dispersion on phosphorus loads transported to Ashumet Pond are discussed in the "Sensitivity Simulations" section.

Hydrologic Boundary Conditions

Boundary conditions are listed in table 3. The northern boundary is assigned a leaky boundary condition and uses the approximate location of the 60-ft water-table contour from Masterson and Walter (2000) for the fixed head. This boundary condition specifies a fixed head of 18.3 m at a distance of 1,700 m from the boundary (X = -2,300 m). Heads on the leaky boundary will depend on flow conditions within the model domain, and the flux of water through the boundary will depend on (1) the head gradient between the boundary and the fixed head at the specified distance and (2) a specified hydraulic conductivity of 1.06×10^{-3} m/s.

The southern boundary also is assigned a leaky boundary condition and uses the approximate location of the 40-ft contour from Masterson and Walter (2000) for the fixed head. For the base-case model, the fixed head is 12.19 m at a distance of 800 m downgradient from the southwest corner of the grid (head = 12.19 m at X = 1,800 m, Y = -1,200 m), varying linearly to a distance of 1,300 m downgradient from the boundary at Y = 0 m (head = 12.19 m at X = 2,300 m, Y = 0 m). Thus, the fixed head is specified downgradient at an angle relative to the boundary of the model grid from Y = -1,200 m to Y = 0 m. The fixed head is parallel to the boundary of the model grid from Y = 0 m to Y = 400 m, and the distance to the fixed head is defined to be 1,300 m from the boundary (X = 2,300 m). The hydraulic conductivity associated with this boundary is 1.06×10^{-3} m/s.

Ashumet Pond is represented as a set of constant-head nodes in the southeast corner of the model grid. Constant-head nodes are defined at an elevation of Z = 7.5 m to Z = 15 m in a zone extending from X = 600 m to X = 1,000 m, and from Y = 0 m to

Y = 400 m. All nodes with X > 600 m, Y > 0 m, and X > 7.5 m (the nodes exclusively within Ashumet Pond) were also defined to be inactive. All constant-head nodes are associated with Ashumet Pond and, therefore, flux to Ashumet Pond is equal to the flux through the active constant-head nodes of the model.

No-flow boundaries are applied to the eastern and the stair-stepped western edges of the model grid, including both X and Y faces of the stair steps. The bottom of the model grid is also a no-flow boundary. No water enters or leaves the system through the no-flow boundaries.

The top of the model grid is a flux boundary, through which rainfall recharges the aquifer. The recharge rate from rainfall is specified to be 1.8×10^{-3} m/d (0.66 m/yr).

A flux boundary condition accounts for recharge of sewage effluent through the disposal beds; during the period of use of a bed for sewage-effluent disposal, the flux of rainwater for the bed is ignored. The disposal beds, numbered 1 through 25 (figs. 1 and 4), have been loaded for different periods of time and at different rates over the course of operation of the sewage-treatment plant. The history of total plant discharge and usage of the individual disposal beds is uncertain. The total discharge from the plant is estimated to have varied from 400 to 6,000 m^3/d (0.1 to 1.5 Mgal/d) over the course of operation. For simplicity in the model, the disposal beds were defined as five 100-m × 100-m areas. The current best estimate of the history of the plant discharge and loading for these five areas is listed in table 4 (D.R. LeBlanc, U.S. Geological Survey, written commun., 2001).

Chemical Initial and Boundary Conditions

At the beginning of the simulation period (initial condition), the aquifer was assumed to be filled with uncontaminated ground water of the composition given in table 5. All water flowing into the model domain through the northern boundary also had the composition of uncontaminated ground water. For the base-case calculations, only dissolved oxygen and nitrate were considered in the recharge from rainfall to the aquifer within the model domain (table 5). Finally, the composition of treated sewage effluent (table 5) was assumed to be constant throughout the operation of the plant, except that dissolved oxygen was assumed to be absent prior to the sewage plant upgrade in 1984 (base-case only) and present from 1984 through 1995.

Chemical Reactions in the Sewage Plume

Determination of loads of phosphorus transported to Ashumet Pond was the primary objective of this study. However, phosphorus sorbs strongly to aquifer sediments, and furthermore, phosphorus sorption is dependent on pH. Thus, when the fate and transport of phosphorus are simulated, it is important to consider not only phosphorus sorption, but any other reactions in the sewage plume that affect pH. The reactions for the base-case model of the sewage plume included phosphorus sorption, cation sorption, iron- and manganese-oxyhydroxide mineral equilibria, and decomposition of dissolved organic carbon. Additional reactions were included in the revised model to account

Table 4. Estimated loading of disposal beds during the period of sewage disposal

[Each set of beds was assumed to be 10,000 square meters in area for modeling. Beds 17 and 18 were assumed never to have been used. Mgal/d, Million gallons per day]

Time period	Total sewage-effluent load (Mgal/d)	Flux (meter per day)				
		Beds 1–4	Beds 5–8	Beds 9–12	Beds 13–16	Beds 19–25
1936–40	0.1	0.037	0.0	0.0	0.0	0.0
1941–45	1.5	.114	.114	.114	.114	.114
1946–55	.3	.023	.023	.023	.023	.023
1956–70	1	.126	.126	.126	.0	.0
1971–77	.4	.05	.05	.05	.0	.0
1978–83	.3	.114	.0	.0	.0	.0
1984–95	.2	.0	.038	.038	.0	.0

Table 5. Solution compositions for uncontaminated ground water, treated sewage effluent, and rainwater

[Concentrations are in micromoles per liter, unless otherwise noted. TDIC, total dissolved inorganic carbon; TOC, total organic carbon; °, degree; --, constituent not included in rainwater]

Constituent or physical property	Uncontaminated ground water	Treated sewage effluent	Rainwater
pH, standard units	5.6	6.0	5.0
Temperature, °C	14	14	25
Dissolved oxygen	125	[a]125	220
Calcium	29	335	--
Magnesium	31	170	--
Sodium	200	2,100	--
Potassium	10	240	--
Sulfate	86	290	--
Chloride	[b]158	[b]1,361	--
Nitrate	0	1,050	10
Ammonium	0	180	--
Phosphorus	0	190	--
Iron	0	4.5	--
Manganese	.64	.4	--
TOC	0	1,600	--
TDIC	28	1,200	--

[a]Treated sewage effluent was assumed to have no dissolved oxygen prior to 1984.

[b]Chloride was adjusted to achieve charge balance in the solution.

for accumulation of non-desorbable phosphorus in the sediments, reaction of sorbed organic carbon, and irreversible denitrification. The major chemical reactions used in the base-case and revised models (excluding equilibrium among aqueous species) are listed in table 6.

Sorption Reactions

The equilibrium constants and sorption sites determined from results of the sorption/desorption-column experiments were used to describe phosphorus and cation sorption for the three-dimensional reactive-transport model. The numbers of sorption sites for phosphorus and cations in the aquifer were adjusted according to the difference in porosity between the experimental columns and the aquifer as follows:

$$sites_{aq} = sites_{col}\left(\frac{P_{col}}{1-P_{col}}\right)\left(\frac{1-P_{aq}}{P_{aq}}\right)$$

$$= sites_{col}\left(\frac{0.33}{0.67}\right)\left(\frac{0.61}{0.39}\right) = 0.77 sites_{col}, \qquad (3)$$

where $sites_{aq}$ and $sites_{col}$ represent the number of aquifer and column sorption sites, and P_{aq} and P_{col} represent the porosities of the aquifer and the column.

Iron and Manganese Minerals

Amorphous ferric hydroxide and pyrolusite were assumed to be present in the same amounts as described for the column-experiment modeling above; the minerals react to equilibrium unless completely removed by dissolution.

Organic Decomposition Reactions

The decomposition of organic carbon derived from the sewage effluent is an important reaction in the aquifer. The decomposition reactions cause large suboxic and anoxic zones within the plume (Walter and others, 1996). The most reducing conditions in the aquifer are represented by an anoxic zone with large iron concentrations between beds 5-8 and Ashumet Pond. A constant concentration of dissolved organic carbon of 1,600 µmol/L was assumed to be present in the sewage effluent throughout the period of sewage disposal. This assumed concentration of dissolved organic carbon in the effluent is consistent with measured values from the 1980s (LeBlanc, 1984). In the simulations, the dissolved organic carbon was consumed by a first-order kinetic reaction with a rate constant of 1.0×10^{-7} s^{-1}. The most thermodynamically favored electron acceptor available—dissolved oxygen, nitrate, pyrolusite, or iron oxyhydroxide—was reduced as the organic carbon was oxidized. Results of PHAST simulations with this rate constant and dissolved organic-carbon concentration show a zone of iron concentrations of approximately 300 µmol/L about

Table 6. Major chemical reactions used in reactive-transport simulations

[*C*, concentration; *k*, rate constant; *SI*, saturation index; *DOC*, dissolved organic carbon; | | indicates absolute value]

Reaction	Reaction type	Equation
Phosphorus sorption	Equilibrium	$SiteOH + PO_4^{3-} + 2H^+ = SiteHPO_4^- + H_2O$
Phosphorus-sorption site protonation	Equilibrium	$SiteOH + H^+ = SiteOH_2^+$
Phosphorus-sorption site deprotonation	Equilibrium	$SiteOH = SiteO^- + H^+$
Cation sorption	Equilibrium	$Cation\_siteOH + Cat^{x+} = Cation\_siteOCat^{x-1} + H^+$
Cation-sorption site protonation	Equilibrium	$Cation\_siteOH + H^+ = Cation\_siteOH_2^+$
Cation-sorption site deprotonation	Equilibrium	$Cation\_siteOH = Cation\_siteO^- + H^+$
$Fe(OH)_3$(amorphous)	Equilibrium	$Fe(OH)_3(a) + 3H^+ = Fe^{+3} + 3H_2O$
Pyrolusite	Equilibrium	$MnO_2 + 4H^+ + 2e^- = Mn^{+2} + 2H_2O$
Decomposition of dissolved organic carbon (DOC), reactant is CH_2O	Kinetic	$Rate = -kC_{DOC}$
Decomposition of sorbed organic carbon, reactant is CH_2O (post cessation)	Kinetic	$Rate = -k_{O_2} C_{O_{2,aq}} - k_{NO_3} C_{NO_{3,aq}}$
Vivianite precipitation and dissolution, reactant is $Fe_3(PO_4)_2$	Kinetic	$Rate = -kC_{PO_4}\left(\frac{SI_{vivianite}}{1 + \lvert SI_{vivianite}\rvert}\right)$
Strengite precipitation and dissolution, reactant is $FePO_4$	Kinetic	$Rate = -kC_{PO_4}\left(\frac{SI_{strengite}}{1 + \lvert SI_{strengite}\rvert}\right)$
Removal of dissolved N_2 (prevents N_2 reoxidation to nitrate), reactant is N_2	Kinetic	$Rate = -kC_{N_{2,aq}}$

150 m downgradient of disposal beds 5-8 in 1993, which is consistent with the field measurements shown in Walter and others (1996, p. 32). However, the simulated iron zone extends all the way to Ashumet Pond, which is contrary to field observations.

After cessation of sewage disposal, the introduction of dissolved organic carbon ceased, but sorbed organic carbon present in the aquifer continues to react. From measurements of oxygen demand of contaminated sediments, a concentration of 41,500 µmol/L of sorbed organic carbon was estimated for the zone between the disposal beds and Ashumet Pond (Richard Smith, U.S. Geological Survey, written commun., 2001). After cessation of sewage disposal, sorbed organic carbon was allowed to react with dissolved oxygen and nitrate in the simulation until these electron acceptors were consumed. First-order kinetics were used for both electron acceptors with the rate constants 1.0×10^{-7} s^{-1} and 1.5×10^{-7} s^{-1}, respectively. (The assignment of different values was done inadvertently but the difference is not significant.) This formulation of organic-carbon decomposition reactions for the period following cessation of sewage disposal consumes oxygen and nitrate, but does not allow for the consumption of iron oxyhydroxide and the maintenance of an iron zone in the aquifer;

however, the effect of additional organic decomposition that maintains an iron zone was evaluated in the sensitivity simulations.

Iron Phosphate Minerals

Although not included in the base-case model, one of the sensitivity simulations of the base-case model and the revised model allowed for kinetically controlled precipitation and dissolution of ferric phosphate (strengite) and ferrous phosphate (vivianite) minerals. The rate equations for these two minerals are listed in table 6.

Irreversible Denitrification

Thermodynamic equilibrium between nitrate and dissolved nitrogen was specified for the base-case simulation and all sensitivity simulations. Dissolved nitrogen is relatively inert, however, so that denitrification is simulated more realistically as an irreversible process. Irreversible denitrification was implemented in the revised model and will be discussed in the "Revised Model" section.

Fitting Surface-Sorption Parameters to Sorption/Desorption Experimental Data

Results of the sorption/desorption column experiments are plotted in figure 5 with PHAST simulation results. Parameter estimation was used to fit the number of phosphorus-sorption sites and the log K for the phosphorus-sorption reaction (eq. 1) that were used in this model. The log K for surface protonation also was fit using parameter estimation, but the model was insensitive to the log K for surface deprotonation, which was then arbitrarily assigned a value of -7.0.

The initial plateau in the measured pH at small numbers of pore volumes (~pH 5, fig. 5) could not be fit with phosphorus sorption alone. It was assumed that a set of cation-sorption reactions must account for the shape of the pH curve at small numbers of pore volumes; however, the data were insufficient to fit the number of sorption sites and to discriminate among the major cations. Only two parameters were fit for cation sorption: (1) the number of cation-sorption sites and (2) a single equilibrium constant that applied to the sorption reactions for all cations—Ca, Mg, Na, K, NH_4, Fe, and Mn—of the form:

$$Cation\_siteOH + Cat^{x+} = Cation\_siteOCat^{x-1} + H^{+}, \quad (4)$$

where $Cation\_site$ represents a cation-sorption site, and Cat^{x+} is a cation with charge x.

It was difficult to fit all parameters simultaneously; log K values were dependent on the number of sorption sites, such that increasing the number of sites and decreasing the log K tended to give a similar fit. The parameters listed in table 7 were all fit simultaneously (except for the log K for deprotonation), and they produced the simulation results for both columns that are shown in figure 5. The parameter fit is not unique, and depends somewhat on starting values for the parameter estimation. Equally good fits could be found with variations of the parameters. However, the number of cation sites from table 7 (23,000 µmol/L) corresponds to a cation-exchange capacity of approximately 0.5 meq/100 g sediment, which is consistent with estimates of cation-exchange capacity for these sediments (Ceazan and others, 1989). With the number of cation sites fixed at 23,000 µmol/L, an optimum fit to the data could be found only if the number of phosphate sorption sites was within the range of 2,000 to 3,500 µmol/L. For this range in number of phosphate sorption sites, the corresponding variations in the fit of log K values for phosphate sorption and site protonation were both approximately 1.2 log units. The fit values for the phosphate parameters were not sensitive to the cation parameters.

Sensitivity Simulations

The sensitivity of the three-dimensional reactive-transport model to selected parameters was investigated by individually perturbing model parameters or sets of model parameters that described a single process. The effects of 11 parameters and parameter sets were simulated, and for each perturbation, the load of phosphorus transported to Ashumet Pond was calculated for each year of the simulation. Only the relative effect of the parameter change on the load transported to Ashumet Pond should be considered because of the preliminary nature of the base-case set of model parameters.

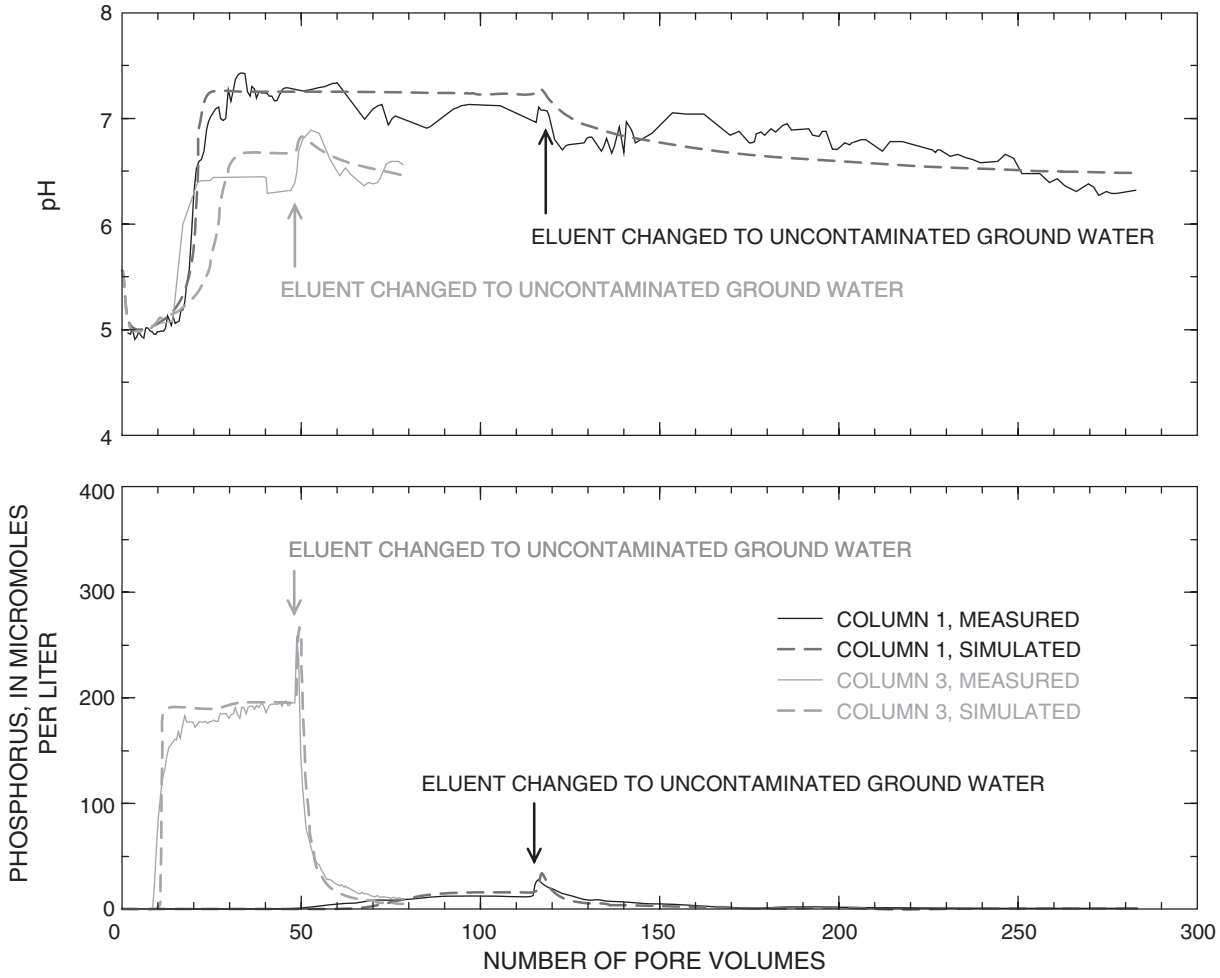

Figure 5. Results of column experiments of phosphorus sorption and desorption on Cape Cod sediments and results of reactive-transport simulations based on fitted parameters. Influent phosphorus concentration in column 1 was 16 micromoles per liter and in column 3 was 196 micromoles per liter.

Usually, a parameter value was increased and decreased to evaluate its effect; however, this pattern was not followed in the following four cases: (1) The sensitivity of the model to the maintenance of an iron zone following cessation of sewage disposal was investigated by adding a kinetic reaction that allowed sufficient sorbed organic carbon to react to generate approximately 150 µmol/L dissolved iron. This process was specified to occur for the 60 years following the cessation of sewage disposal in a 900-m × 300-m × 25-m-thick zone that contained the disposal beds and extended to Ashumet Pond. (2) The sensitivity of the model to the fixed head of the southern leaky boundary was investigated by lowering the head, but not by raising the head. (3) The effect of numerical dispersion was investigated by halving the time step and X- and Y-direction grid size (Z direction unchanged), which should halve the horizontal numerical dispersivity to approximately 30 m. (4) The sensitivity of the model to sequestration of phosphorus in a non-desorbable form was investigated by including equilibrium and kinetic mineral reactions with iron-phosphate minerals.

Iron-phosphate colloids have been identified near the disposal beds (Gschwend and Reynolds, 1987), and phosphate sorption may ultimately lead to surface precipitation of solids or solid solutions (Dzombak and Morel, 1990). To examine the effects of incorporating phosphorus into the sediments in a non-sorbing form, strengite (ferric phosphate) and vivianite (ferrous phosphate) were included in the

Table 7. Parameters derived from fitting sorption/desorption column experiments

[Site, phosphorus-sorption site. Cation-site, cation-sorption site. µmol/L, micromoles per liter]

Parameter	Value
log K: $SiteOH + PO_4^{3-} + 2H^+ = SiteHPO_4^- + H_2O$ (eq. 1)	26.7
log K: $Cation\_siteOH + Cat^{x+} = Cation\_siteOCat^{x-1} + H^+$ (eq. 4)	-1.8
Sorption sites for PO_4^{3-}, µmol/L	3,000
Sorption sites for cations, µmol/L	23,000
log K: $SiteOH + H^+ = SiteOH_2^+$ and $Cation\_siteOH + H^+ = Cation\_siteOH_2^+$	4.1
log K: $SiteOH = SiteO^- + H^+$ and $Cation\_siteOH = Cation\_siteO^- + H^+$	-7.0

model as equilibrium phases (log K values defined by *wateq4f.dat*, Parkhurst and Appelo, 1999). These phases were not present at the beginning of the simulation, but could form when the solution became saturated and subsequently continue to precipitate or redissolve to maintain equilibrium. A kinetic formation of these minerals was implemented with a rate expression that was formed as the product of the following: a rate constant (2.3×10^{-8} s^{-1}), the concentration of dissolved phosphorus, and a Monod factor based on the saturation index of the mineral with half-saturation constant of 1.0 (unitless). This rate constant produced a distribution of strengite at the time of cessation that was greatest at the disposal beds and decreased downgradient to near zero in about 400 m. The same rate constant was used for vivianite.

The base-case and perturbed values for parameters are listed in table 8 for 11 sensitivity-simulation cases. Figure 6 shows the phosphorus load transported to Ashumet Pond for simulations with perturbed parameters compared to the load calculated for the simulation with the base-case parameters. For most simulations the load transported to Ashumet Pond has a peak around 1970 and second peak around 2005.

The timing of the first peak is generally consistent among the calculations, but is delayed slightly by decreasing the cation-sorption log K (case 3) or increasing the number of cation-sorption sites (case 4). Decreasing the cation-sorption log K relative to the base case produces initial conditions with nearly twice as many uncharged OH sites that can participate in deprotonation reactions to maintain the pH at lower values for a longer period of time than the base case. The lower pH values cause stronger sorption and smaller dissolved phosphorus concentrations; similarly, increasing the number of cation-sorption sites allows a longer period of low pH initially, during which phosphorus is sorbed more strongly.

The magnitude of the first peak decreases or increases with adjustment to most parameters. The following perturbations tend to decrease the magnitude of the first peak in phosphorus load transported to Ashumet Pond: increasing the phosphorus-sorption constant (case 1), increasing the number of phosphorus-sorption sites (case 2), decreasing the concentration of dissolved organic carbon in sewage effluent (case 5), decreasing the rate constant for decomposition of dissolved organic carbon (case 6), lowering the specified head for the southern leaky boundary (case 8), decreasing the phosphorus concentration in sewage effluent (case 9), and formation of iron-phosphate minerals (case 10).

The magnitude of the first peak appears to be most sensitive to the concentration of dissolved organic carbon in the sewage effluent, the concentration of phosphorus in the sewage effluent, and the formation of iron-phosphate minerals. Doubling the concentration of dissolved organic carbon in the sewage effluent (case 5) causes intense iron dissolution and sulfate reduction in the simulation, which has not been observed in the plume. These redox reactions generate pH values as high as 9.5, which are also inconsistent with field measurements. The high pH values have the effect of diminishing the sorption of phosphorus and increasing the load of phosphorus transported to Ashumet Pond. Halving the concentration of dissolved organic carbon (case 5) causes the iron zone not to form in the simulation, and causes pH values of about 5

Table 8. Base-case and perturbed values for sensitivity simulations with the three-dimensional reactive-transport model

[X, X-direction (fig. 4); Y, Y-direction (fig. 4); Z, Z-direction (vertical); P, phosphorus; m, meter; µmol/L, micromoles per liter; s^{-1}, per second; --, no second sensitivity simulation for this case]

Case	Parameter or Process	Base case	Value 1	Value 2
1	P sorption constant (log K, eq. 1)	26.7	27.2	26.2
2	P sorption sites, µmol/L	[a]2,300	4,600	1,150
3	Cation-sorption constant (log K, eq. 4)	-1.8	-0.8	-2.8
4	Cation-sorption sites, µmol/L	[a]18,000	36,000	9,000
5	Dissolved organic carbon in sewage effluent, µmol/L	1,600	3,200	800
6	First-order rate constant for dissolved organic carbon, s^{-1}	1.0×10^{-7}	2.0×10^{-7}	0.5×10^{-7}
7	Generation of iron zone following cessation of sewage disposal	no[1]	yes[2]	--
8	Specified head for southern leaky boundary, m	12.19	11.19	10.19
9	P concentration in sewage effluent, µmol/L	190	285	95
10	Non-desorbable phosphorus	none	Strengite and vivianite equilibrium	Kinetic formation of strengite and vivianite[3]
11	Numerical dispersivity, m	~60	~30	--
	Node spacing X, m	50	25	--
	Node spacing Y, m	50	25	--
	Node spacing Z, m	2.5	2.5	--
	Time step, year	0.5	0.25	--

[a] Number of sites is adjusted from values in table 7 to account for the difference in porosity.

[1] Sufficient organic carbon reacted to consume oxygen and nitrate in a 900 × 300 × 25-m zone containing the disposal beds and extending to Ashumet Pond.

[2] 200 micromoles of organic carbon per liter of water reacted kinetically to consume oxygen and nitrate, and generate approximately 150 µmol/L dissolved iron. This reaction was applied in a 900 × 300 × 25-m zone containing the disposal beds and extending to Ashumet Pond.

[3] Rate equations for strengite and vivianite were $Rate = -kC_{PO_4}\left(\frac{SI}{1+|SI|}\right)$, where $k = 2.3 \times 10^{-8}$, C_{PO_4} is the total dissolved phosphorus concentration, and *SI* is the saturation index for the mineral.

within the plume. These low pH values also are inconsistent with field measurements, but have the effect of increasing the sorption of phosphorus and decreasing the load of phosphorus transported to Ashumet Pond. The concentration of phosphorus in the sewage effluent has a direct effect on the loads of phosphorus transported to Ashumet Pond; increased phosphorus concentration leads directly to increased loads transported to Ashumet Pond and the reverse for decreased phosphorus concentration (case 9). Equilibrium with iron-phosphate minerals essentially sequesters all phosphorus in mineral phases within a short distance of the disposal beds (case 10); in this case, simulated small concentrations of phosphorus within the aquifer are inconsistent with large measured concentrations of phosphorus downgradient of the disposal beds. With the specified kinetic formation of iron-phosphate minerals, ferric phosphate accumulates near the disposal beds and ferrous phosphate accumulates in the large-iron-concentration zone, but phosphorus still discharges to Ashumet Pond. The load of phosphorus transported to Ashumet Pond is then sensitive to the kinetic-rate formulation—the simulated phosphorus load may vary from near zero for fast rates of iron-phosphate mineral formation (producing near-equilibrium conditions), up to the base-case results for slow rates (no mineral formation). Kinetic formation of iron-phosphate minerals has a greater effect on the first peak in phosphorus load than on the second peak.

The timing of the second peak in phosphorus load transported to Ashumet Pond does not appear to be affected by any of the parameter perturbations and occurs around 2005. The magnitude of the second peak appears to be most sensitive to four parameters or processes: (1) Increasing the number of phosphorus-sorption sites (case 2) tends to decrease the second peak in phosphorus load transported to Ashumet Pond. The number of sorption sites for phosphorus is uncertain by at least a factor of two, and additional

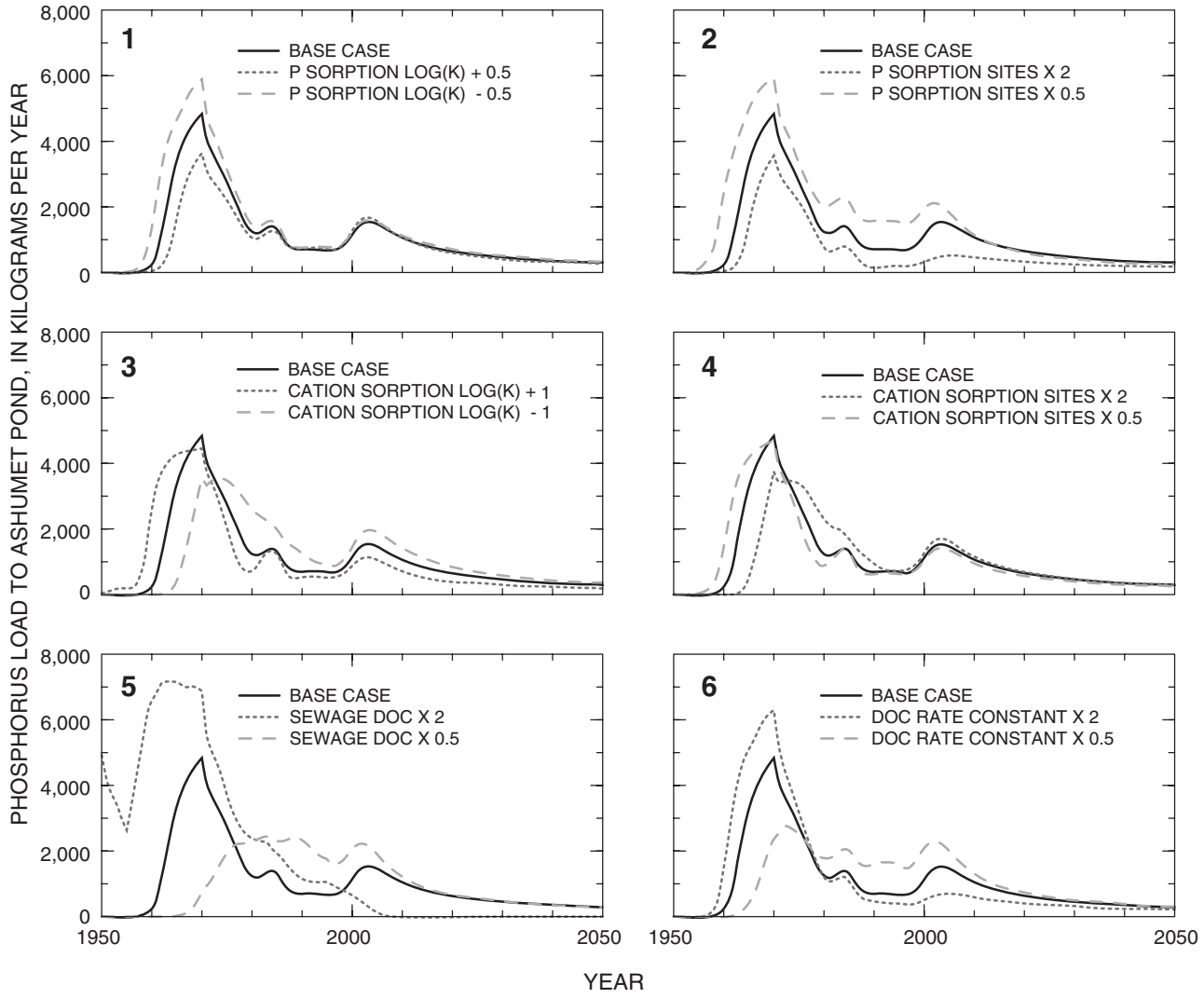

Figure 6. Sensitivity of phosphorus load transported to Ashumet Pond to variation in selected reactive-transport model parameters.

simulations in the "Revised Model" section indicate that the number of sites could be larger. (2) Maintenance of the iron zone following cessation of sewage disposal (case 7) tends to increase the second peak in phosphorus load transported to Ashumet Pond. Measurements of oxygen demand for the contaminated sediments indicate that hundreds of pore volumes of water are needed to consume the sediment oxygen demand. However, the extent to which iron oxyhydroxides will be reduced in the process of oxidizing the organic carbon (the cause of the oxygen demand) is unknown. (3) Allowing more water to flow out across the southern boundary (decreasing the specified head for the leaky boundary, case 8) causes a decrease in the second peak in phosphorus load transported to Ashumet Pond. The relative flow of water out across the southern boundary compared to flow of water to Ashumet Pond is not well constrained, but additional simulations in the "Revised Model" section indicate that the plume in the Ashumet Valley may be better represented if more water is allowed to flow out across the southern leaky boundary. (4) Rapid formation of iron-phosphate minerals (equilibrium, case 10) nearly eliminates phosphorus loads transported to Ashumet Pond.

In addition to the physical and chemical processes, the simulation results include the effects of numerical dispersion. Ideally, the grid and time step of

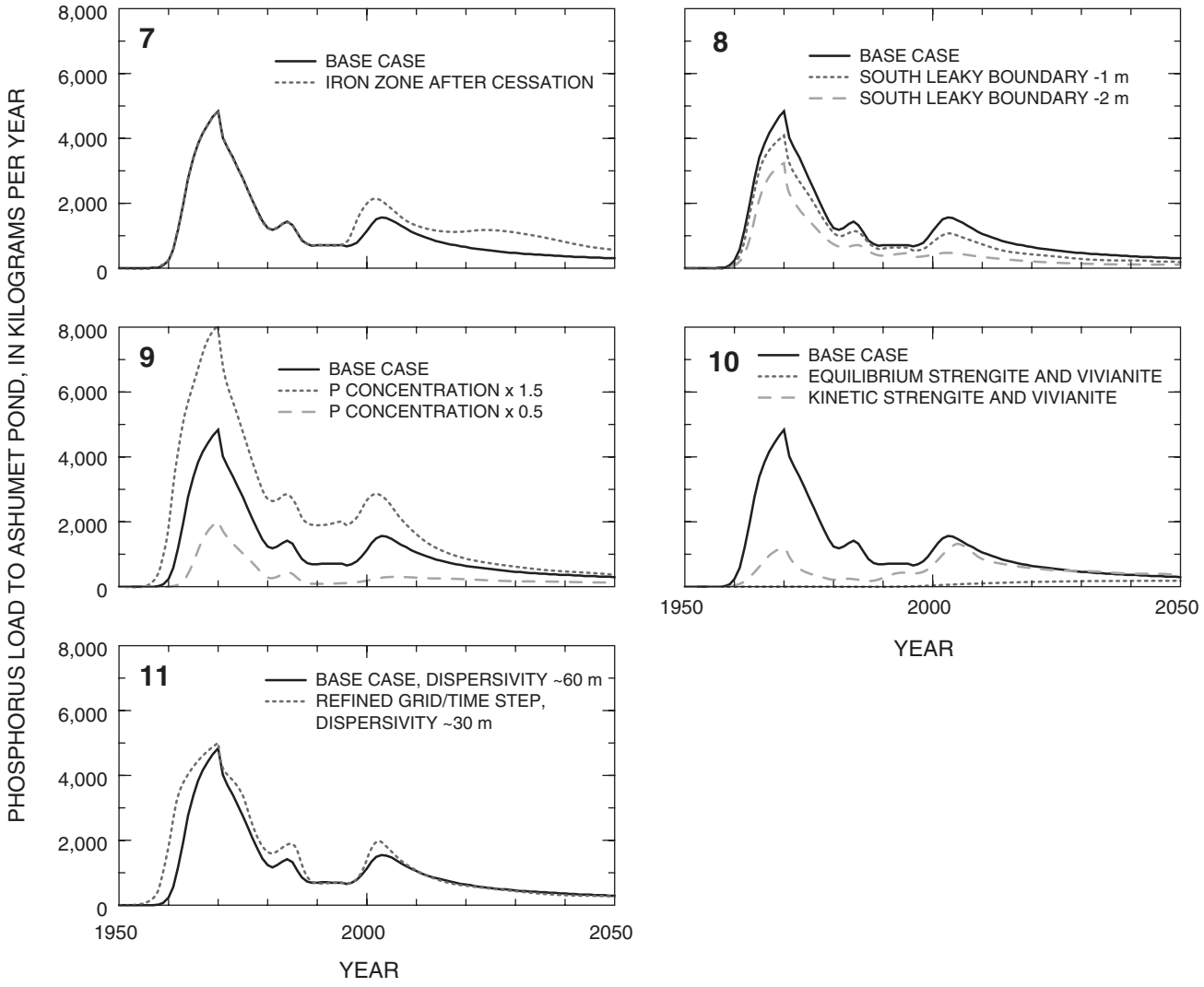

Figure 6. Sensitivity of phosphorus load transported to Ashumet Pond to variation in selected reactive-transport model parameters—*Continued.*

the model are refined until the effects of numerical dispersion are less than the physical dispersion that is simulated. Unfortunately, limitations in computer memory and computer processing time preclude refinement of the model grid and time step to the point of grid and time-step convergence, that is, to the point that no change in results occurs with further refinement of the grid and time step. The base-case model was run with a refined grid and decreased time step (table 8). The dispersivity for this refined grid and time step is estimated to be 30 m, compared to 60 m for the original mesh and time step. The results for the refined grid are similar to the results for the coarse grid (fig. 6, case 11), but with somewhat increased loads for the last two peaks. Further refinement of the grid could change the peak loads substantially; however, the pattern of decreasing loads after about 2005 does not appear to be sensitive to numerical dispersion.

Revised Model

In this section, several of the base-case parameters are adjusted to develop a revised model that better simulates the available data. The results of the sensitivity simulations for the base-case model are used to provide qualitative interpretations for the changes in phosphorus load transported to Ashumet Pond that are simulated by the revised model.

Modifications to the Base-Case Model

By considering additional field and experimental data collected in 1996 and 1999, and reconsideration of chemical processes, the revised model was developed to account for additional processes that are evident in the aquifer, to refine estimates of model parameters, and to finalize estimates of the load of phosphorus transported to Ashumet Pond. Four processes that were not present in the base-case modeling are implemented in the revised model: (1) organic-carbon and oxygen-demand accumulation on the aquifer sediments, (2) irreversible denitrification of nitrate, (3) non-desorbable phosphorus accumulation on the aquifer sediments, and (4) rapid reaction of aquifer sediments with rainwater that infiltrates the aquifer. This section also provides justification for adjusting some of the model parameters used in the base-case modeling, specifically, the head assigned to the southern model boundary, the number of phosphorus-sorption sites, and the oxygen concentrations in the sewage effluent during the first 50 years of disposal. Revisions to the base-case model are summarized in table 9.

Sorption and Subsequent Reaction of Organic Carbon

Over the period of sewage disposal, a large amount of organic carbon accumulated on the aquifer sediments. Measurements of total oxygen demand range from 2.1 to 12.1 µmol of O_2 per g dry sediment in the area downgradient of the disposal beds (Richard Smith, U.S. Geological Survey, written commun., 2001), with a general trend of decreasing oxygen demand with distance downgradient. Assuming 4,150 g of sediment per liter of water, each volume of aquifer containing one liter of water has from 9,000 to 50,000 µmol of oxygen demand and requires 35 to 200 pore volumes of air-saturated water (approximately 250 µmol/L of O_2) to satisfy this oxygen demand. Thus, with flow time from the

Table 9. Comparison of parameters and processes for base-case and revised models

[P, phosphorus; m, meter; µmol/L, micromoles per liter; s^{-1}, per second]

Parameter or process	Base-case model	Revised model
Sorb organic carbon during sewage disposal, react sorbed organic carbon following cessation of sewage disposal	no	yes
Irreversible denitrification	no	yes
Kinetic formation of non-desorbable phosphorus (strengite and vivianite, table 6)	no	yes
Infiltration at top of aquifer	rain	background water
Generation of iron zone following cessation of sewage disposal	no	no
P sorption constant (log K, eq. 1)	26.7	26.7
P sorption sites, µmol/L	2,300	3,450
Cation-sorption constant (log K, eq. 4)	-1.8	-1.8
Cation-sorption sites, µmol/L	23,000	23,000
Dissolved oxygen concentration in sewage effluent, 1936–83, µmol/L	0	250
First-order rate constant for conversion of dissolved nitrogen to non-reactive dissolved species, s^{-1}	0	1.16×10^{-7}
P concentration in sewage effluent, 1935–83, µmol/L	190	380
Rate constant for conversion of dissolved phosphorus to non-desorbable phosphorus (strengite and vivianite rate expressions, table 6), s^{-1}	0	1.16×10^{-8}
Dissolved organic carbon in sewage effluent, µmol/L	1,600	1,600
First-order rate constant for dissolved organic carbon, s^{-1}	1.0×10^{-7}	1.0×10^{-7}
Sorbable organic carbon in sewage effluent, µmol/L	0	1000
First-order rate constant for sorbable organic carbon, 1936–95, s^{-1}	0	1.16×10^{-8}
First-order rate constant for consumption of electron acceptors following cessation of sewage disposal, 1996–2055. Reaction consumes sorbed organic carbon, s^{-1}	0	1.16×10^{-8}
Specified head for southern leaky boundary, m	12.19	10.19

disposal beds to Ashumet Pond on the order of 4 years, anoxic conditions are likely to persist downgradient from the disposal beds for many decades following cessation of sewage disposal.

To simulate the process of accumulation of oxygen demand within the aquifer, an additional pool of organic carbon was added to the sewage effluent, which represented that part of the organic carbon that sorbed on the sediment during disposal of sewage effluent from 1936 through 1995. The concentration of sorbable organic carbon was specified to be 1,000 μmol/L in the sewage effluent, which sorbed by first-order reaction with rate constant 1.16×10^{-8} per second. This concentration and rate constant produced maximum sorbed organic carbon concentrations of 16,000 μmol/L after 60 years of sewage-effluent disposal; the sediment oxygen demand corresponding to this accumulation of sorbed organic carbon is also 16,000 μmol/L.

After cessation of sewage disposal, the model includes kinetic reactions that decrease the sorbed organic carbon concentration as the oxygen in the invading background water is consumed. For each mole of oxygen consumed, one mole of sorbed organic carbon is oxidized; the rate of consumption is first order with respect to the dissolved oxygen concentration. The presence of sorbed organic carbon is required for the process to continue.

Irreversible Denitrification

Thermodynamic equilibrium between nitrate and dissolved nitrogen was specified for the base-case modeling. Field data indicate that dissolved nitrogen is formed by denitrification within the plume as organic carbon is consumed; further reduction of nitrate to ammonium is not apparent. However, in the simulations, dissolved nitrogen within the plume mixed with dissolved oxygen outside the plume by the process of dispersion, and dissolved nitrogen reoxidized to nitrate, with a concomitant decrease in pH. Because dissolved nitrogen is relatively inert and unlikely to reoxidize, denitrification is simulated more realistically as an irreversible process. Irreversible denitrification was implemented in the revised model by removing dissolved nitrogen from the system as it formed from denitrification and adding an equal amount of a new dissolved nitrogen species that could not reoxidize to nitrate in the presence of oxygen. The removal of dissolved nitrogen was modeled as a first-order decay with rate constant 1.16×10^{-7} s^{-1}; the new non-reactive dissolved nitrogen species was produced at an equal rate. The rate constant for these reactions was sufficient to remove all of the dissolved nitrogen essentially as soon as it was formed.

Non-Desorbable Phosphorus

Experiments with contaminated sediments from the aquifer show that not all of the phosphorus can be removed by desorption. Even after repeated rinsing with pH-10 water, most of the phosphorus is retained by the sediment. Total non-desorbable phosphorus ranges from about 0.5 to 8 μmol/g of sediment, or about 2,000 to 35,000 μmol/L of water in the aquifer.

Formation of a large amount of non-desorbable phosphorus in the aquifer requires a greater input of phosphorus into the system, and accordingly, the concentration of phosphorus in the sewage effluent for the period 1936 through 1983 for the revised model was increased to 380 μmol/L from the base-case concentration of 190 μmol/L. This increase in concentration is justified, in part, by the large pool of sorbed phosphorus in the sediments, and, in part, by the use of high-phosphate detergents within this time period.

The revised model implemented the kinetic reactions for ferric phosphate (strengite) and ferrous phosphate (vivianite) minerals used in the sensitivity simulations (case 10, fig. 6). The combination of the increased concentration of phosphorus in the sewage effluent through 1983 and the kinetic reactions produced concentrations of strengite up to 7,000 μmol/L and vivianite up to 1,600 μmol/L. Simulation results indicate that most of the strengite forms immediately downgradient of the disposal beds, whereas vivianite tends to form in and downgradient from the iron zone.

Infiltration at the Surface of the Aquifer

The base-case model recharged dilute nitric acid (pH 5) into the aquifer to simulate the infiltration of rainwater (table 5). However, the reactive surfaces in the model were initialized to be in equilibrium with the uncontaminated ground-water composition (table 5). Reaction of the dilute infiltration water with the pre-equilibrated surfaces caused a pH higher than 6 in the shallow part of the aquifer throughout the simulation. The pH measured in the shallow aquifer is

approximately 5.5, which is similar to the pH of the background water. Thus, for the revised model, the background-water composition was used for recharge in place of rainwater. It is assumed that rainwater reacts rapidly in the shallow part of the aquifer to achieve a composition similar to the uncontaminated background water (table 5).

Leaky Boundary Condition for the Southern Boundary

By using the specified concentration of chloride in the sewage effluent (1,361 μmol/L, table 5) and the prescribed loading history, the total mass of chloride applied through the disposal beds is 2,200,000 kg for all simulations. All of this chloride must eventually leave the model domain, either through the constant-head nodes that represent Ashumet Pond or through the leaky boundary at the southern edge of the domain. In the base-case model, 90 percent of the sewage-derived chloride left the domain through nodes that represent Ashumet Pond, and about 10 percent, or 200,000 kg, left the domain through the southern boundary. This small flux of chloride through the southern boundary appears to be inconsistent with the development of the large sewage plume in Ashumet Valley (fig. 1).

To estimate the mass of chloride contributed by sewage effluent to the Ashumet Valley plume, a mass accounting for chloride in Ashumet Valley was done. A total of 328 chloride-concentration data from 1994 from sites throughout Ashumet Valley (Savoie and LeBlanc, 1998) were assembled. These data were interpolated to a regular, three-dimensional grid, from which the mass of chloride in the Valley was estimated by means of a zero moment routine (R.L. Naff, U.S. Geological Survey, written commun., 2002). Any excess chloride above the background concentration of 10 mg/L was assumed to be contributed by the sewage effluent. The total mass of chloride in the valley contributed by the sewage effluent is estimated to be 2,000,000 to 2,500,000 kg. This range of estimate still has a large uncertainty because of the sparsity of spatial coverage of the data, the selection of a constant background concentration, and because of the difficulty of accurately interpolating and integrating the data over a large region. However, the base-case calculation of only 200,000 kg of chloride entering Ashumet Valley appears to be an order of magnitude too small.

The parameter in the model that effectively distributes the flow between Ashumet Pond and the southern boundary is the specified head for the leaky southern boundary condition. By lowering the head for the leaky southern boundary condition, more water will flow through the southern boundary and less water will flow to Ashumet Pond. By lowering the head associated with the boundary by two meters (to 10.19 m), the mass of chloride transported through the southern boundary is about 1,100,000 kg. Although still smaller than the estimate of sewage-derived chloride derived from the measured concentration data in the Ashumet Valley, it is within a factor of two of the estimate, and it accounts for nearly half of the sewage-derived load of chloride in the simulation. Further lowering the head of the boundary condition generates head gradients that are significantly greater than are currently measured in the flow system. The revised model uses a 2-m reduction in the head associated with the leaky southern boundary, which is a compromise between allowing sufficient sewage-derived chloride to flow into Ashumet Valley and maintaining head gradients that approximate water-level measurements.

Number of Sorption Sites

Model parameters for sorption processes were fit from sorption/desorption column experiments on uncontaminated sediments. A column experiment desorbing phosphorus from contaminated sediments also was run (see “Methods” section). This desorption column experiment was simulated by using the parameters derived from the sorption/desorption column experiments.

The main difficulty in simulating the phosphorus desorption experiment was in the definition of initial conditions. The core material was obtained from site S469 at the southern edge of the disposal beds in April 2000, approximately 4.5 years after cessation of sewage disposal. To account for the period of time between cessation of sewage disposal and sample collection, the initial composition of the reactive surfaces in the column were modified as follows: first, the surfaces were brought to equilibrium with treated sewage effluent (table 5), and second, the surfaces were flushed with 15 pore volumes of uncontaminated ground water (table 5). The simulated phosphorus concentrations in equilibrium with the surface

compositions following this procedure were similar to the initial phosphorus concentrations released during the phosphorus desorption experiment (fig. 7).

The simulation results for the desorption column experiment generated with base-case parameters for sorption reactions are shown in figure 7. The general trend in phosphorus concentration in the leachate is captured by the simulation, although simulated phosphorus concentrations are consistently smaller than the experimental data. It is plausible that the number of sorption sites may vary within the aquifer and may vary as a result of reactions in the sewage plume, such as sorption of organic carbon or precipitation of additional iron oxyhydroxide surfaces. Surface areas measured on aquifer sediments varied by a factor of two within the same sediment core (Fuller and others, 1996), which implies that the number of sorption sites could also vary by at least this extent within the aquifer. Increasing the number of surface sites in the simulation of the desorption experiment tends to increase the phosphorus concentrations in the leachate because a larger pool of desorbable phosphorus is defined by the initial conditions. A factor-of-two increase in the number of sites, while maintaining the same log K for the phosphorus-sorption reaction, tends to produce simulated concentrations similar to measured concentrations for 25 to 150 pore volumes, although simulated phosphorus concentrations are larger than measured concentrations for the first 25 pore volumes and smaller than measured concentrations for the last 50 pore volumes (fig. 7).

The number of sites for the revised model was increased by a factor of 1.5, splitting the difference between the number of sites fit from the sorption/desorption experiments and the apparent need for a greater number of sites in the desorption experiment.

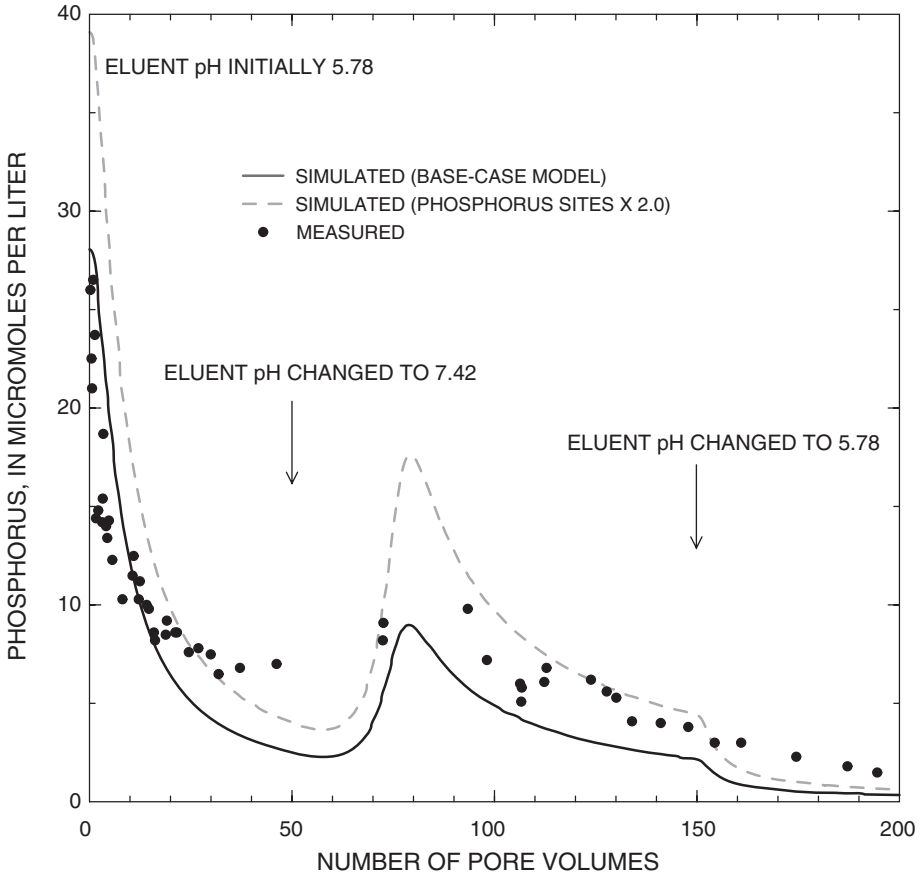

Figure 7. Measured and simulated phosphorus concentrations for a column desorption experiment on a sediment core from the sewage-contaminated zone of the aquifer.

Oxygen Concentration in Sewage Effluent

The oxygen concentration in the sewage effluent for the base-case model was arbitrarily set to zero for the period 1936–83. For the revised model, a constant oxygen concentration in the sewage effluent (250 µmol/L) was used for the entire period of sewage effluent disposal. The oxygen is consumed in the oxidation of organic carbon, which produces carbon dioxide. The additional input of carbon dioxide tends to buffer the pH at lower values for a longer period of time. The overall effect of the additional oxygen on the simulations is relatively small.

Comparison of Measured and Simulated Phosphorus Concentrations

Reactive-transport simulations provide concentrations of phosphorus at each active node in the model grid for each year of the period of simulation. Simulation results from the revised model are compared to measured phosphorus concentrations in space and time.

Phosphorus Distribution in 1993

As a test of the revised model, simulated phosphorus concentrations were compared with a comprehensive set of measured phosphorus concentrations in the aquifer from August through November 1993 (Walter and others, 1996). Figure 8 shows contours of the measured phosphorus concentration from 1993; maximum concentrations were used for sites that had samples from multiple depths. Figure 8 also shows contours of simulated phosphorus concentration for the end of 1993; for consistency, maximum concentration was used for each vertical set of nodes. The simulated phosphorus concentrations are similar to the measured phosphorus concentrations, both in location and in magnitude of the peak concentrations downgradient from the disposal beds. In the simulation, the easternmost large concentrations are derived from beds 1-4, which were the only beds used during the period 1978–83; those beds were not used thereafter. The westernmost large concentrations in the simulation are derived from beds 5–12, which were the only beds used during the period 1984–95. The location of the observed phosphorus concentration peaks and the magnitude of the measured phosphorus concentrations are reproduced by the reactive-transport simulations, but the maximum simulated phosphorus concentrations southeast of beds 1–4 are larger (270 µmol/L) than maximum measured concentrations in this area (180 µmol/L). The simulated large phosphorus concentrations southeast of beds 1-4 extend all the way to Ashumet Pond, but the measured large concentrations decrease toward the Pond. The measured concentrations show smaller, narrower lobes of large phosphorus concentrations, which may be due to selective use of individual disposal beds (compared to the equal distribution of sewage effluent to groups of disposal beds simulated in the model), to the small dispersivity of the aquifer, or to inadequate spatial coverage of the ground-water sampling locations.

Phosphorus at Site S469

Decreases in phosphorus concentrations have been measured in wells near the disposal beds since the cessation of sewage disposal. Site S469 is at the edge of disposal beds 5-8, and a multilevel sampler at this location was sampled in July 1996 and July 1999. During that period, phosphorus concentrations decreased significantly at altitudes greater than -10 m. Measured phosphorus concentrations in multilevel sampler S469M1 and phosphorus concentrations simulated with the revised model for the vertical set of nodes nearest to the location of disposal beds 5-8 are shown in figure 9. The simulated concentrations are consistent with a marked decrease in measured phosphorus concentrations near the disposal beds in the time frame of 3 years. The magnitude of the simulated concentration change also is consistent with the magnitude of the measured concentration change.

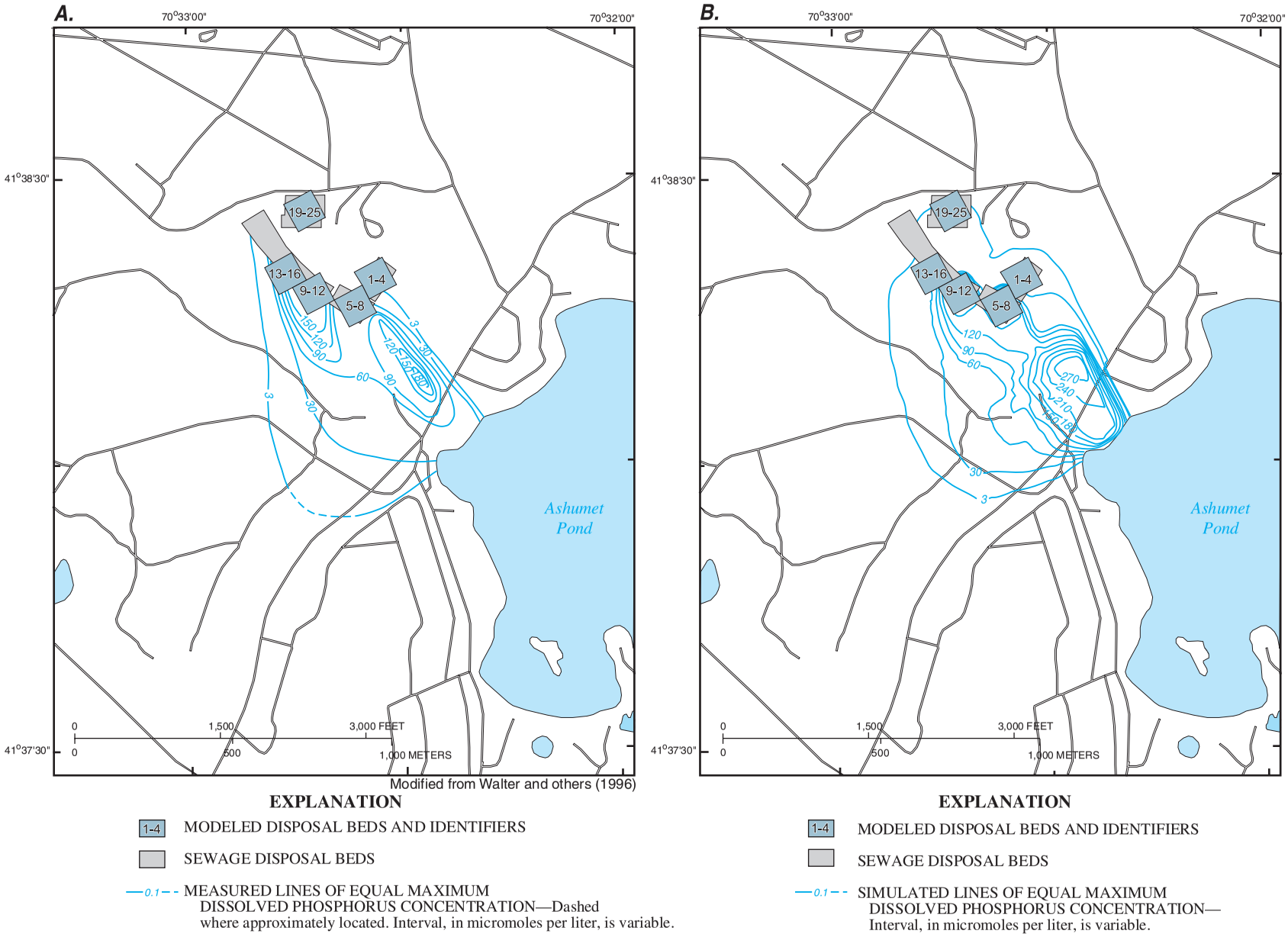

Figure 8. (*A*) Measured and (*B*) simulated phosphorus concentrations in ground water from August to November 1993 near Ashumet Pond, Massachusetts.

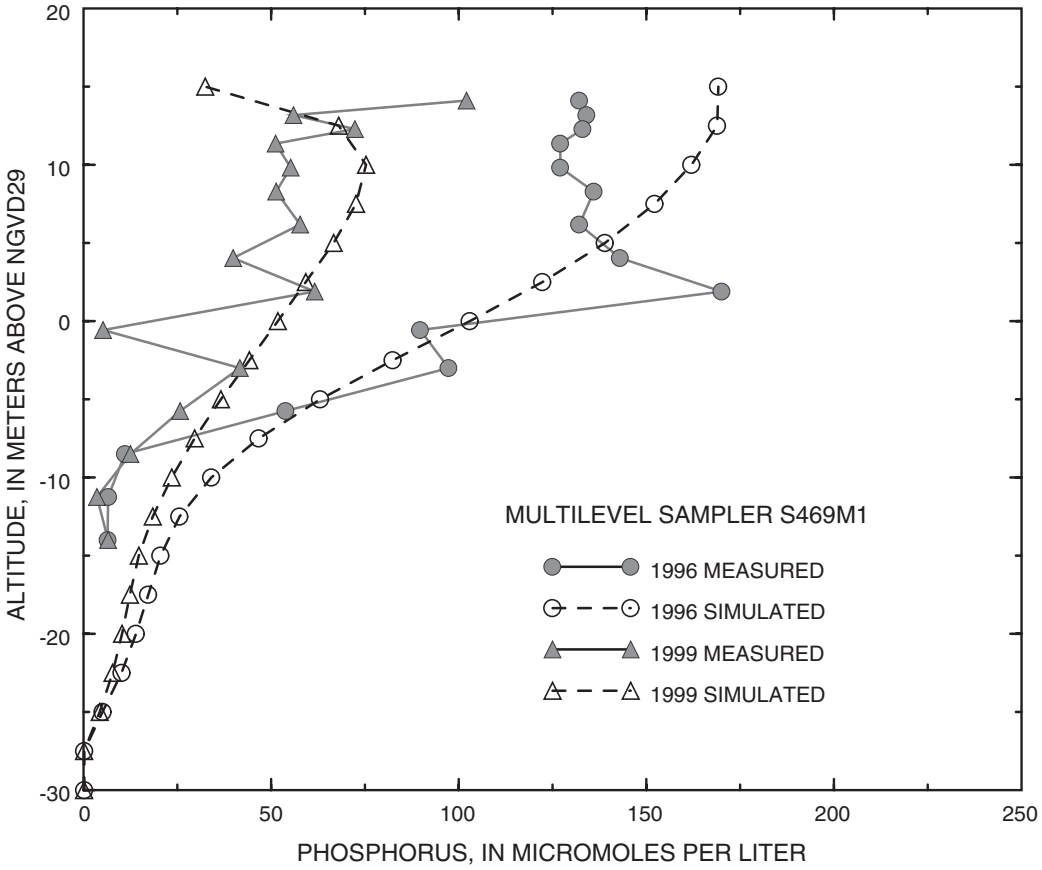

Figure 9. Measured phosphorus concentrations in July 1996 and July 1999 in multilevel sampler S469M1 and simulated phosphorus concentrations for the vertical set of nodes nearest to the location of disposal beds 5–8.

Transport of Phosphorus to Ashumet Pond

The timing and sequence of the peaks in phosphorus load transported to Ashumet Pond are determined by a combination of effects related to phosphorus concentration in the sewage effluent, the sequence of loading the disposal beds, and the chemical response of the aquifer to the loading of sewage effluent and related chemical reactions. However, several results are consistent for all plausible simulations with parameters from the base-case, sensitivity, and revised-model simulations. First, the earliest substantial phosphorus loads transported to Ashumet Pond are simulated to have occurred in the 1960s, nearly 30 years after the initial use of the disposal beds and 20 years after peak loading of the disposal beds. Second, the simulated phosphorus load transported to Ashumet Pond decreases with time after the 2000–10 time period; however, substantial phosphorus loads continue for decades. And third, the phosphorus load transported to Ashumet Pond is a small fraction of the total phosphorus loaded through the disposal beds. Most of the phosphorus is retained in the aquifer sediment in the sorbed and non-desorbable fractions. Consistent with the sorption/desorption and desorption column experiments, the simulations indicate that this large pool of sediment-bound phosphorus remains sequestered for a long period of time and ultimately maintains small concentrations of dissolved phosphorus in the ground water.

Loads of phosphorus at the disposal beds and the loads of phosphorus transported to Ashumet Pond simulated by using the revised model are plotted in figure 10. For the revised model, the simulated load of phosphorus transported to Ashumet Pond increased in the late 1960s and remained approximately constant until 1985. The constant load over this period of time is markedly smaller than the corresponding peak in load calculated for the base-case

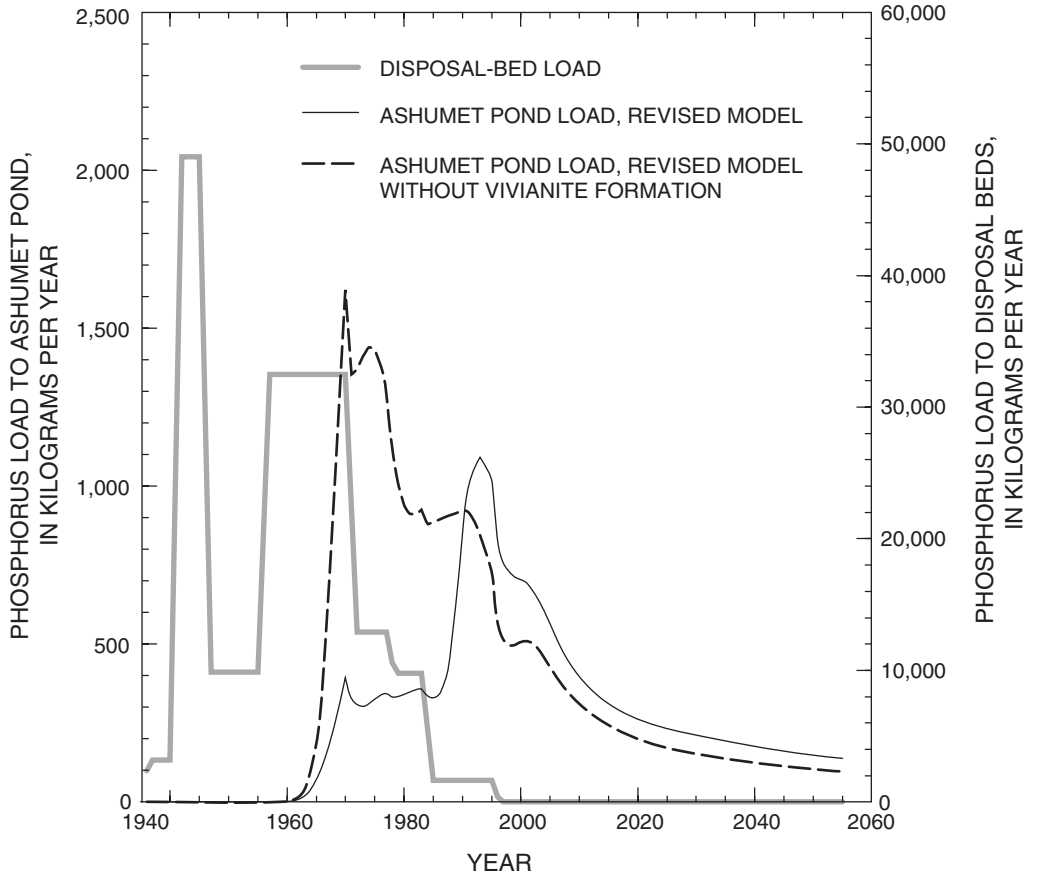

Figure 10. Simulated load of phosphorus transported to Ashumet Pond, Massachusetts, and estimated load of phosphorus to disposal beds during the period 1936 to 2055, calculated with revised model parameters and revised model parameters excluding vivianite formation.

model for this period of time (fig. 6), even though a larger concentration of phosphorus was introduced with the sewage effluent in the revised model over most of the period of sewage disposal. The larger input in phosphorus simulated in the revised model does not cause larger loads to be transported to Ashumet Pond compared to the base-case model because (1) the amount of phosphorus transported away from the Pond toward Ashumet Valley is greater because of the lower head for the southern leaky boundary, (2) the uptake of phosphorus by sorption is greater because of the increased number of phosphorus-sorption sites, and (3) the transfer of phosphorus to non-desorbable phosphorus sequesters phosphorus in the sediment.

The load of phosphorus transported to Ashumet Pond is especially sensitive to the formation of vivianite. A simulation using the revised model, but without vivianite formation, shows larger loads of phosphorus transported to Ashumet Pond during the period 1965–85 (fig. 10) compared to smaller loads in the revised model with vivianite formation. In the absence of vivianite formation, however, the larger phosphorus loads transported to Ashumet Pond are sustained by larger phosphorus concentrations. Without vivianite formation, the western lobe of large phosphorus concentrations (>90 μmol/L near disposal beds 8–16) extends to Ashumet Pond and the northern part of Ashumet Valley (not shown), which is inconsistent with smaller measured phosphorus concentrations in this area in 1993 (see fig. 8 for location of western lobe of large measured phosphorus concentrations).

The revised model simulates a peak in phosphorus load transported to Ashumet Pond between 1990 and 2010, and although the calculations are better suited to qualitative interpretations, the maximum load during this period is estimated to be about 1,000 kg/yr. The phosphorus in this peak is derived mostly from

loading the eastern disposal beds (beds 1–4) prior to 1984. The location of the maximum measured phosphorus concentrations was approximately 350 m downgradient from beds 1–4 in 1993 (fig. 8). This downgradient location demonstrates the transport of phosphorus over this distance during a period of at least 10 years, the time since the beds were used. However, differences between the simulated and measured phosphorus concentrations downgradient of beds 1–4 in 1993 (fig. 8) indicate that the timing and magnitude of the peak in phosphorus load transported to Ashumet Pond (fig. 10) may not be accurately predicted by the revised model. The simulated phosphorus concentrations are larger than the measured concentrations, and the large simulated concentrations extend to a greater distance downgradient toward Ashumet Pond than the large measured concentrations. These differences between the simulated and measured phosphorus concentrations indicate that the simulation results describe a larger peak in phosphorus load transported to Ashumet Pond that occurs and dissipates more quickly than actually occurs in the aquifer.

Limitations of the Revised Model

Of the many uncertainties involved in developing the revised model, the following appear to have the greatest effects on the load of phosphorus transported to Ashumet Pond:

- **The loading history of the beds**—The concentration of phosphorus in the sewage effluent directly affects the load of phosphorus transported to Ashumet Pond. In addition, the history of disposal-bed usage—the specific beds and rates of disposal, particularly for individual beds on the eastern side—is critical to the estimation of phosphorus loads transported to Ashumet Pond.
- **The mechanism by which phosphorus is incorporated into the non-desorbable sediment fraction**—The chemical form of the non-desorbable phosphorus is largely unknown, but extremely important. The long-term stability of the non-desorbable phosphorus is uncertain, although column experiments indicate it is not readily released. The kinetic expressions describing the incorporation of the non-desorbable form into the sediment are plausible and result in a reasonable match between simulated and measured phosphorus concentrations, but are otherwise poorly constrained. In the revised model, the presence or absence of vivianite formation switches the period of peak phosphorus load transported to Ashumet Pond from the 1990s to the 1970s (fig. 10). Although the loads after 1990 are not greatly affected, the uncertainty makes it difficult to assess whether current loads are greater or less than the loads transported in previous decades.
- **The description of the flow system**—Small changes to the model flow system can distribute the phosphorus loaded on the western disposal beds (beds 5–25) either to Ashumet Pond or to Ashumet Valley. The flow system is much more dynamic than simulated in the revised model, with seasonal variations in water level in Ashumet Pond and ground-water flow direction in the aquifer; however, a model that accounts for the dynamics of the flow system is beyond the scope of this report.
- **The extent of decomposition of organic carbon following cessation of sewage disposal**—In the revised model, decomposition occurs only to the extent that dissolved oxygen and nitrate are consumed in the presence of sorbed organic carbon. Sulfate reduction and methanogenesis have not been observed during the period of sewage disposal and are unlikely to be initiated following cessation of sewage disposal, when the reactivity of sorbed organic carbon is expected to decline. However, it is possible that organic decomposition will proceed further than the revised model allows. Reductive dissolution of iron- (and manganese-) oxyhydroxide minerals has been observed in the core of the sewage plume, but no reaction is included in the revised model to maintain reductive dissolution of iron and manganese minerals following cessation of sewage disposal. Iron and manganese oxyhydroxide dissolution will tend to raise the pH and increase the mobility of phosphorus.

Simultaneously, increased iron concentrations may tend to sequester phosphorus in ferrous phosphate mineral phases. Thus, the extent of reductive dissolution of iron-oxyhydroxide minerals following cessation of sewage disposal and related effects on phosphorus load transported to Ashumet Pond are difficult to assess.

- **Cation-sorption reactions**—These reactions are poorly defined, but affect the buffering of pH in ground water, which affects the sorption and mobility of phosphorus in the aquifer.

SUMMARY AND CONCLUSIONS

The subsurface transport of phosphorus introduced by the disposal of treated sewage effluent at the Massachusetts Military Reservation on western Cape Cod was simulated with a three-dimensional reactive-transport model. The simulation was used to estimate the load of phosphorus transported to Ashumet Pond during sewage-treatment-plant operation—1936 to 1995—and for 60 years following cessation of sewage disposal. The model accounted for spatial and temporal changes in water discharge from the sewage-treatment plant, ground-water flow, transport of associated chemical constituents, and a set of chemical reactions, including phosphorus sorption on aquifer materials, dissolution and precipitation of iron- and manganese-oxyhydroxide and iron-phosphate minerals, organic carbon sorption and decomposition, and cation sorption.

The three-dimensional reactive-transport model combined flow and transport calculations with chemical reactions. The flow and transport in the aquifer was modeled by using parameters consistent with previous flow and transport models of this area of Cape Cod, except that numerical dispersion was much larger than the physical dispersion estimated in previous studies.

A base-case model was developed by using measured phosphorus concentrations from the aquifer and results from laboratory column experiments. A series of sensitivity simulations was made by varying the parameters and processes that were used in the base-case model. A revised model was developed by consideration of sensitivity-simulation results, comparison with additional laboratory column experimental results, comparison with field data, and inclusion of additional chemical processes.

Chemical reactions were included in the revised model to simulate the major reactions in the aquifer. The surface-complexation equilibrium constants and number of sorption sites for phosphorus and cations were adjusted in a reactive-transport model to fit the pH and phosphorus concentrations measured in column experiments. Iron- and manganese-oxyhydroxide minerals were assumed to react to equilibrium. Rates of organic carbon decomposition were adjusted to match the location and iron concentrations in the anoxic iron zone within the sewage plume. Additional reactions were incorporated in the model to account for the accumulation of sorbed organic carbon and non-desorbable phosphorus in aquifer sediments and to model denitrification as an irreversible process.

All plausible simulations with the base-case and revised models indicate that the phosphorus load transported to Ashumet Pond was minimal before 1965; the load transported to Ashumet Pond decreases following the period 2000–10, but is substantial for many decades; and most of the phosphorus introduced through the disposal beds resides in the aquifer sediments. The current calculations indicate a peak in phosphorus discharge to Ashumet Pond of about 1,000 kg/yr during the 1990s; however, comparisons of modeled phosphorus concentrations with measured concentrations from samples taken in 1993 indicate that the peak in phosphorus load transported to Ashumet Pond may be larger and moving more quickly in the model simulations than is evident in the aquifer.

Simulation results from the revised three-dimensional reactive-transport model are consistent with the current understanding of the loading history, laboratory experimental data, and measured concentrations in water samples from the aquifer. However, large uncertainties are associated with the loading of the sewage beds, the flow system, and the chemistry and sorption characteristics in the aquifer. As an example of the large uncertainties, the revised model indicates a small load of phosphorus during 1965–85,

but this small load is particularly sensitive to model parameters that specify flow conditions and the chemical process by which non-desorbable phosphorus is incorporated in the sediments. The uncertainties are sufficient that it is difficult to determine whether loads of phosphorus transported to Ashumet Pond in the 1990s were greater or less than loads during the previous two decades. The revised model adequately reproduces the spatial distribution of phosphorus concentrations measured in 1993, the magnitude of changes in phosphorus concentration in a vertical profile of the aquifer near the disposal beds after cessation of sewage disposal, the observed iron zone in the sewage plume, the approximate flow of treated sewage effluent into Ashumet Valley, and laboratory column data for phosphorus sorption and desorption.

REFERENCES CITED

Barber, L.B., II, 1990, Geochemical heterogeneity in a glacial outwash aquifer—Effect of particle size and mineralogy on sorption of nonionic organic solutes: Boulder, University of Colorado, Department of Geological Science, Ph.D. dissertation, 238 p.

Ceazan, M.L., Thurman, E.M., and Smith, R.L., 1989, Retardation of ammonium and potassium transport through a contaminated sand and gravel aquifer—The role of cation exchange: Environmental Science and Technology, v. 23, no. 11, p. 1402–1408.

Coston, J.A., Fuller, C.C., and Davis, J.A., 1995, Pb^{2+} and Zn^{2+} adsorption by a natural aluminum- and iron-bearing surface coating on an aquifer sand: Geochimica et Cosmochimica Acta, v. 59, no. 17, p. 3535–3547.

Dzombak, D.A., and Morel, M.M., 1990, Surface complexation modeling: New York, John Wiley and Sons, 393 p.

Fishman, M.J., and Friedman, L.C., 1985, Methods for determination of inorganic substances in water and fluvial sediments: Techniques of Water-Resources Investigations of the U.S. Geological Survey, book 5, chap. 1, p. 477–478.

Fuller, C.C., Davis, J.A., Coston, J.A., and Dixon, Eleanor, 1996, Characterization of metal adsorption variability in a sand and gravel aquifer, Cape Cod, Massachusetts, U.S.A: Journal of Contaminant Hydrology, v. 22, no. 3-4, p. 165–187.

Garabedian, S.P., LeBlanc, D.R., Gelhar, L.W., and Celia, M.A., 1991, Large-scale natural-gradient tracer test in sand and gravel, Cape Cod, Massachusetts—2. Analysis of spatial moments for a nonreactive tracer: Water Resources Research, v. 27, no. 5, p. 911–924.

Gschwend, P.M., and Reynolds, M.D., 1987, Monodisperse ferrous phosphate colloids in an anoxic groundwater plume: Journal of Contaminant Hydrology, v. 1, no. 3, p. 309–327.

Harbaugh, A.W., and McDonald, M.G., 1996, User's documentation for MODFLOW-96, an update to U.S. Geological Survey Modular Finite-Difference Ground-Water Flow Model: U.S. Geological Survey Open-File Report 96-485, 56 p.

Kipp, K.L., Jr., 1997, Guide to the revised heat and solute transport simulator—HST3D: U.S. Geological Survey Water-Resources Investigations Report 97-4157, 149 p.

LeBlanc, D.R., 1984, Sewage plume in a sand and gravel aquifer, Cape Cod, Massachusetts: U.S. Geological Survey Water-Supply Paper 2218, 28 p.

LeBlanc, D.R., Garabedian, S.P., Hess, K.M., Gelhar, L.W., Quadri, R.D., Stollenwerk, K.G., and Wood, W.W., 1991, Large-scale natural-gradient tracer test in sand and gravel, Cape Cod, Massachusetts—Experimental design and observed tracer movement: Water Resources Research, v. 27, no. 5, p. 895–910.

LeBlanc, D.R., Hess, K.M., Kent, D.B., Smith, R.L., Barber, L.B, Stollenwerk, K.G., and Campo, K.W., 1999, Natural restoration of a sewage plume in a sand and gravel aquifer, Cape Cod, Massachusetts, *in* Morganwalp, D.W., and Buxton, H.T., eds., U.S. Geological Survey Toxic Substances Hydrology Program—Proceedings of the Technical Meeting, Charleston, South Carolina, March 8–12, 1999—Volume 3, Subsurface Contamination from Point Sources: U.S. Geological Survey Water-Resources Investigations Report 99-4018C, p. 245–259.

Masterson, J.P., and Walter, D.A., 2000, Delineation of ground-water recharge areas, western Cape Cod, Massachusetts: U.S. Geological Survey Water-Resources Investigations Report 00-4000, 1 pl.

McDonald, M.G., and Harbaugh, A.W., 1988, A modular three-dimensional finite-difference ground-water flow model: Techniques of Water-Resources Investigations of the U.S. Geological Survey, book 6, chap. A1, variously paged.

Parkhurst, D.L., and Appelo, C.A.J., 1999, User's guide to PHREEQC (Version 2)—A computer program for speciation, batch-reaction, one-dimensional transport, and inverse geochemical modeling: U.S. Geological Survey Water-Resources Investigations Report 99-4259, 312 p.

Parkhurst, D. L., Engesgaard, Peter, and Kipp, K.L., 1995, Coupling the geochemical model PHREEQC with a 3D multi-component solute transport model, *in* Program and Abstracts: State College, PA, V.M. Goldschmidt Conference, May 24–26, 1995, p. 77–78.

Parkhurst, D.L., and Kipp, K.L., 2002, Parallel processing for PHAST—A three-dimensional reactive-transport simulator, *in* Hassanizadeh, S.M., Schlotting, R.J., Gray, W.H., and Pinder, G.F., eds., Computational methods in water resources, v. 2, Developments in Water Science, n. 47: Amsterdam, The Netherlands, Elsevier, p. 711–718.

Poeter, E.P., and Hill, M.C., 1999, UCODE, A computer code for universal inverse modeling: Computer in Geosciences, v. 25, p. 457–462.

Savoie, Jennifer, and LeBlanc, D.R., 1998, Water-quality data and methods of analysis for samples collected near a plume of sewage-contaminated ground water, Ashumet Valley, Cape Cod, Massachusetts, 1993–94: U.S. Geological Survey Water-Resources Investigations Report 97-4269, 208 p.

Stollenwerk, K.G., 1995, Modeling the effects of variable ground-water chemistry on adsorption of molybdate: Water Resources Research, v. 31, no. 2, p. 347–357.

Stollenwerk, K.G., 1996, Simulation of phosphate transport in sewage-contaminated groundwater, Cape Cod, Massachusetts: Applied Geochemistry, v. 11, p. 317–324.

Stollenwerk, K.G., and Parkhurst, D.L., 1999, Modeling the evolution and natural remediation of a ground-water sewage plume, *in* Morganwalp, D.W., and Buxton, H.T., eds., U.S. Geological Survey Toxic Substances Hydrology Program—Proceedings of the Technical Meeting, Charleston, South Carolina, March 8–12, 1999, Volume 3, Subsurface Contamination from Point Sources: U.S. Geological Survey Water-Resources Investigations Report 99-4018C, p. 371–381.

Walter, D.A., Rea, B.A., Stollenwerk, K.G., and Savoie, Jennifer, 1996, Geochemical and hydrologic controls on phosphorus transport in a sewage-contaminated sand and gravel aquifer near Ashumet Pond, Cape Cod, Massachusetts: U.S. Geological Survey Water-Supply Paper 2463, 89 p.